Thermal Regimes and Snowpack Relations of Periglacial Talus Slopes, Sierra Nevada, California, U.S.A.

Authors: Millar, Constance I., D. Westfall, Robert, and Delany, Diane L.

Source: Arctic, Antarctic, and Alpine Research, 46(2) : 483-504

Published By: Institute of Arctic and Alpine Research (INSTAAR), University of Colorado

URL: https://doi.org/10.1657/1938-4246-46.2.483

Arctic, Antarctic, and Alpine Research, Vol. 46, No. 2, 2014, pp. 483–504

Thermal Regimes and Snowpack Relations of Periglacial Talus Slopes, Sierra Nevada, California, U.S.A.

Constance I. Millar†*
Robert D. Westfall and*
*Diane L. Delany**

*USDA Forest Service, Pacific Southwest Research Station, 800 Buchanan Street W.A.B., Albany, California 94710, U.S.A.
†Corresponding author: cmillar@fs.fed.us

Abstract

Thermal regimes of eight periglacial talus slopes, at contrasting elevations, aspects, and substrates, in the Sierra Nevada, California, had complex microclimatic patterns partially decoupled from external conditions. Over three years, warm seasons showed mean talus matrix temperatures and daily variances lower than surfaces and cooler than free-air; talus surface and matrix positions low in the taluses were colder than higher positions, yielding highly positive altitudinal temperature differentials; ground surface temperatures had greater daily extremes than talus positions; and talus matrix temperatures lagged in response to surface temperature changes. Regulating processes in summer include evaporative cooling, cold-air drainage and Balch effect, and shading effects. In the cold season, talus matrices were warmer than surfaces; low talus positions were warmer than high; isothermal zero-curtain periods occurred before snow disappearance; and snow covered talus low positions more often and longer than higher in the taluses, which were often snow-free. Winter thermal processes likely include insulation from snow cover at talus bases, free exchange between talus matrix and external air in the upper talus, and latent heat from thaw-refreezing in late winter. Permanent ice may occur within high elevation talus slopes. Partially decoupled talus thermal regimes provide buffered habitats for mammals such as American pikas and are likely to be important refugia under future warming.

DOI: http://dx.doi.org/10.1657/1938-4246-46.2.483

Introduction

Mountain environments are inherently subject to extreme climates. Under continued anthropogenic warming they are also expected to be at high likelihood of change, with cascading effects on vulnerable ecosystems (Beniston, 2003; Parmesan and Yohe, 2003; Thuiller et al., 2005). Global and regional models, based on expectations that temperatures decrease as elevations increase, project pervasive losses of alpine communities and biota as species migrate upslope tracking favorable climates into the future (Hayhoe et al., 2004). At scales of ecological importance, however, micro- and topographic climate processes are as likely to influence change as are synoptic climates (Daly et al., 2009; Pepin and Lundquist, 2008; Dobrowski, 2010). Current research focuses on the role of topographic and geomorphologic complexity in local-scale thermal regimes that directly affect mountain biota. As some of these appear at least partially decoupled from ambient regional climates, they likely exert much different effects on plants and animals than expected under models that don't include these processes.

Periglacial landforms that consist of coarse material such as rock glaciers, block fields, and talus slopes are ubiquitous in mountain regions, especially those that experienced Pleistocene glaciation (Giardino and Vitek, 1988; Barsch, 1996; Curry and Morris, 2004; Sass, 2006). In alpine and arctic periglacial zones, they have been shown to promote and sustain permafrost. Due to partially decoupled thermal regimes that maintain colder than external air temperatures, these features can depress the regional permafrost altitudinal limit by as much as 1000 m (Delaloye and Lambiel, 2005). Because of their importance in controlling the amount and distribution of permafrost, efforts have increased to better understand their internal thermal regimes and how these relate to regional climate, snowpack, and permafrost (Ishikawa, 2003; Sawada et al., 2003; Delaloye and Lambiel, 2005; Juliussen and Humlum, 2008).

Much of the work to date on thermal regimes has focused on rock glaciers, and then mostly on features in Europe and Greenland and in cold regions that receive abundant snowfall (references in Millar et al., 2012). Less effort has focused on thermal regimes of talus slopes (Harris and Pedersen, 1998), in particular in warm regions and temperate latitudes where permafrost or persistent ice is sporadic. In the semi-arid Sierra Nevada of eastern California, rock glaciers, block fields, and talus slopes are common, and many have forms and features that suggest that permanent ice remains embedded within the rocky matrix (Millar and Westfall, 2008). This is undoubtedly the case for rock glaciers that are glaciogenic, that is, derive from clean glaciers having stratified ice that subsequently developed a rock mantle (Clark et al., 1994). The same appears to hold for many Sierran periglacial rock glaciers, that is, those whose internal ice derives from avalanching, snowmelt and freeze-thaw processes, and potentially localized ground permafrost development. Prior work has shown that persistent ice is highly likely in the latter, as indicated by pilot studies that monitored temperature of rock-glacier matrices, as well as very cold temperature and persistence of spring water issuing from these features (Millar et al., 2012). Aside from preliminary explorations of talus slopes in that same study, no systematic investigations have been made on thermal regimes of these features in the Sierra Nevada or elsewhere in the American Southwest region.

OBJECTIVES

The overall goal was to improve understanding of thermal regimes of periglacial taluses in warm-temperate and semi-arid mountains such as the Sierra Nevada. In particular, we sought to elucidate (1) seasonal patterns of temperature and heat transfer

1523-0430/17 $7.00

within talus matrices and between talus and external air, (2) snowpack relationships of talus slopes as they relate to thermal dynamics, (3) altitudinal position effects within taluses, and (4) associations between talus thermal regimes and ambient climates (role of microclimatic processes). We also investigated the effects of elevation, substrate, and slope aspect, as well as interannual variability. In that taluses are critical habitats for mountain mammals such as the American pika (*Ochotona princeps*), and that talus forefields support critical wetland refugia for alpine plants and animals, we hope that improved understanding of talus thermal dynamics will reveal the importance of geomorphology on these unique talus ecosystems (Kubat, 2000), especially in the context of changing climates.

Methods

STUDY SITES

We selected eight taluses in the eastern Sierra Nevada, Mono County, California, two in the East Walker River Watershed and six in the Mono Basin (Table 1, Fig. 1). Of these, four were on north-facing and four on south-facing aspects; two of each aspect were at low elevations (mean, 2403 m) and two at high elevations (mean, 3163 m). Of the four south-facing taluses, one at each elevation was granitic, and one was metamorphic substrate. Although we intended to parallel this contrast for north-facing taluses, we could not find an adequate low-elevation talus on metamorphic substrate, so we selected two low granitic sites. In the study region, granitic rocks derive from Mesozoic arc-related plutons, while metamorphic rocks source from a wide range of dark red, black, and brown metavolcanic and metasedimentary bedrock of diverse ages. Soil and fine-grained clasts were absent from these taluses, which appear to have originated from Pleistocene and Holocene freeze-thaw sorting (French, 2007). Clasts were smaller in the metamorphic taluses (15–50 cm diameter) than in granitic features (50 cm–1.5 m), with the effect that matrix spaces were larger in the latter as well. Talus slope areas averaged 7.9 ha. Steepness varied from low (23%, Greenstone) to moderate gradient (48%, Lundy South), with the angle consistent along the extent of the transects. None of the sites lies directly below cliffs, and the rock debris derived apparently either from long-distance transport or eroded in situ. No evidence exists for avalanching at any of these sites. The specific origin of our study talus slopes, whether through processes related to alpine rockfall (White, 1981), periglacial sorting (Washburn, 1956, 1980), or colluvial boulder deposit and subsequent erosion—especially in dryland regions (Friend et al., 2000—remains uncertain. Nonetheless, the emergence of common end-member talus forms, having at least superficially consistent morphology (Millar and Westfall, 2008), suggests that diverse processes led to convergent landforms.

Sharp boundaries distinguished talus borders from adjacent upland slopes on the talus sides and from vegetated forefields at talus lower bases. The high-elevation sites were primarily in alpine environments, with low shrub and alpine herbaceous plant associations on adjacent slopes and wet meadows in the forefields, which support a diversity of herbaceous wetland plant species (Millar et al., 2014). The low elevation sites were within montane forest communities that included aspen (*Populus tremuloides*; Green Creek [Cr] and Lundy North) and Jeffrey pine-big sagebrush (*Pinus jeffreyi-Artemesia tridentata*; Lundy South, Lee Vining Canyon [Cyn]). Forefields supported aspen (Green Cr and Lundy North) and sagebrush/rabbitbrush (*Ericameria nauseosus*) communities. As of 2013, all taluses were actively occupied by American pikas and served also as habitat for other small to mid-sized montane mammals and their predators (Millar and Westfall, 2010).

FIELD METHODS

We used Maxim (www.maxim-ic.com/products/ibutton/) DS1921 and 1922 iButton instruments to monitor temperature at all sites and positions. Instrument accuracy was set to 0.5 °C, which was

TABLE 1

Locations and environmental context of eight talus fields studied in the central Sierra Nevada, California, and the reference SNOTEL site. Coordinates and elevation are given for the center bottom of the talus slopes. Sites are ordered from north to south within elevation classes.

Site name	Elevation (m)	Aspect	Substrate	Latitude (°N)	Longitude (°W)	Size (ha)
A. Talus Slopes						
Low-Elevation Sites						
Green Cr	2548	S	granitic	38.099	119.293	4.5
Lundy Cyn South	2373	S	metamorphic	38.035	119.214	4.2
Lundy Cyn North	2387	N	granitic	38.025	119.241	10.1
Lee Vining Cyn	2302	N	granitic	37.929	119.181	4.8
High-Elevation Sites						
Virginia Cyn	3234	N	metamorphic	38.044	119.277	13.2
Saddlebag Lk	3143	S	metamorphic	37.984	119.283	17.3
Warren Fk	3163	S	granitic	37.982	119.241	4.5
Greenstone Lk	3110	N	granitic	37.977	119.293	4.4
B. Virginia Ridge						
SNOTEL site	2804	NE	metamorphic	38.077	119.231	

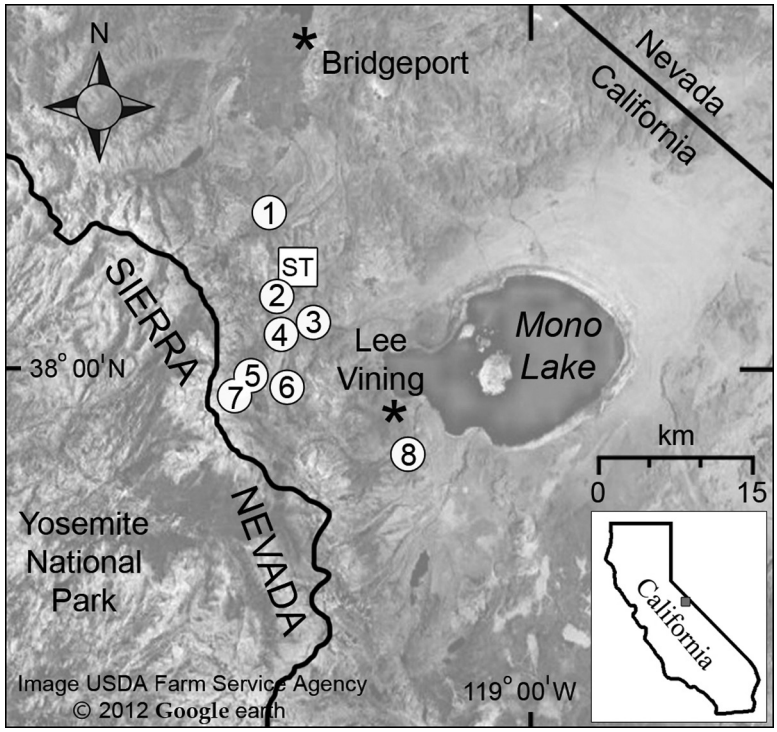

FIGURE 1. Map of the study locations, showing eight talus sites and the USDA–NRCS Virginia Ridge SNOTEL site.

confirmed for a period of two weeks at the beginning of the study by comparing iButton records to a high-resolution thermometer and testing iButtons in diverse thermal conditions. Thermochrons were programmed to record at 4-hr intervals, starting at noon local time on the day they were deployed. We secured the instruments in wire mesh and inserted the mesh in white PVC T-fittings, which had three 2-cm-diameter openings. The PVC fittings served as sun shelters, and allowed airflow to the instrument, while the mesh protected them from small mammals. Wire tethers secured the iButton package to rocks or tree stems depending on position, and also allowed us to place instruments into matrix locations.

In summer 2009, we deployed 30 iButtons at each of the four south-facing taluses in the following arrangement (Fig. 2): iButtons were placed at four positions (forefield, low talus, middle talus, high talus) along four vertical transects that extended from the base of the talus at the forefield up the talus slope ~120 m. The forefield iButton was deployed on the ground surface in shaded vegetation within 2 m of the talus border. Pairs of iButtons were installed at the three equidistant (40 m) talus positions up-transect. At each position, one iButton was installed on the surface of the talus, shaded from direct sun. A second iButton was inserted as near as possible to 1.0 m depth in the matrix. Starting in summer 2010, two iButtons were deployed in shaded canopy, and protected also from ground radiation, at 3 m height on the north side of a tree near the forefield position of the two outside transects. In summer 2010, we deployed 15 iButtons at each of the four north-facing taluses. Because results from the first year on south-facing sites were highly consistent among transects, we reduced by half the total number of iButtons for the north-facing taluses, using two transects and one tree position per talus. For all sites, data were downloaded in the field and instruments reprogrammed in early summer and again in autumn of each year until early autumn 2012, when we terminated the project.

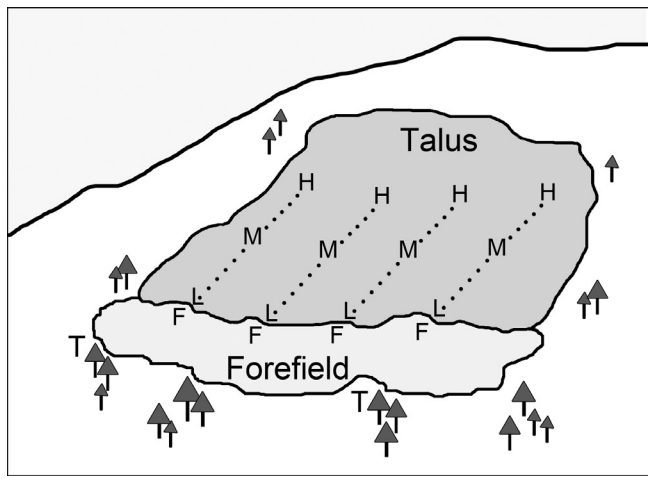

FIGURE 2. Design for deployment of iButtons at talus sites. The four south-facing sites had 30 iButtons positioned along four transects. At each of three positions along the transects (low, mid, high), pairs of surface and matrix thermochrons were deployed. A single iButton was situated on the forefield ground surface in front of each transect, and iButtons were hung in two trees at 3 m height. For the four north-facing sites, 15 iButtons were installed along two transects and in one tree.

TEMPERATURE AND SNOWPACK ASSESSMENTS

Thermochron time-series data were used directly to assess air temperature, indirectly as a proxy to assess snow-cover, and combined to investigate talus heat-transfer processes. Thermochrons in tree canopies provided data for ambient (free-air) temperature (FAT), including mean annual air temperatures

TABLE 2

Abbreviations used in the text for temperatures indicators.

Abbreviation	Temperature indicator
ATD	Altitudinal temperature differential; measure of difference in temperature between elevations within a talus slope, either within the matrix or along the surface. Negative values indicate cooler temperatures at higher elevations.
FAT	Free air temperature, measured at 3.0 m above ground level in tree canopies.
FI	Freezing index.
GST	Ground surface temperature, measured on the talus forefield below the lower talus border.
MAAT	Mean annual air temperature.
TI	Thawing index.
TMT	Talus matrix temperature, measured ~1 m below the talus surface.
TST	Talus surface temperature.

(MAAT), and freezing and thawing indices (FI, TI, respectively; see Table 2 for abbreviation list). FI and TI, indicated as degree days, are calculated as the yearly sum of days with means below 0 °C (freezing degree-days) or above 0 °C (thawing degree-days). The forefield iButton data represented air temperatures at the ground surface (GST; Haeberli, 1973), whereas talus surface and matrix locations provided air temperature specific to the talus landform positions (TST and TMT, respectively). Mean air temperatures were calculated for the cold season (1 October–31 May) and warm season (1 June–30 September) and further subdivided for summer (1 June–30 September), autumn (1 October–31 December), winter (1 January–31 March), and spring (1 April–31 May) in years where data were complete. For each location, we calculated altitudinal temperature differentials (ATD), which is the mean difference in temperatures between low and high positions divided by the elevation difference (upper minus lower) and expressed per 100 m elevation. Negative values indicate that temperature decreases as altitude increases, whereas positive values indicate temperature increases with altitude. Although the processes differ, ATD can be qualitatively compared to the atmospheric lapse rate, which is –0.65 °C per 100 m under standard conditions in mountainous regions, including the Sierra Nevada (Martinec and Rango, 1986; Lundquist and Cayan, 2007).

Low thermal conductivity of snow and its insulating capacity cause GST under a deep snowpack to maintain freezing (0 °C) temperatures with low fluctuation (Haeberli, 1973). We define snow events to have occurred and persisted when GST fell to and remained between 0 and 1 °C (Ishikawa, 2003; Juliussen and Humlum, 2008; Lundquist and Lott,2008). Snow onset dates were identified by an abrupt drop in temperature to freezing, and drop in daily variance. To estimate changes in daily variances in temperatures, we applied generalized autoregressive conditional heteroscedasticity (GARCH) models to the data. We first removed autoregressive trends in the data, then regressed terms of short-memory (p) and long memory (q) (Chatfield, 2004). Models were fit by minimizing Akaike's Information Criterion (AIC) and Schwarz's Bayesian Criterion (SBC) scores (SAS, 2011).

Under shallow snow depths, heat exchange can occur through a snowpack (Haeberli,1973; Hoelzle et al., 1999). In those situations, GST values fluctuate above or below 0 °C with small diurnal fluctuations, reflecting attenuated trends of external ambient air temperature. Snow depths greater than ~0.5 m are required to insulate talus surface relative to a soil surface (Hanson and Hoelzle, 2004; Juliussen and Humlum, 2008). During spring snowmelt, the snowpack loses its insulation capacities by compaction of snow and increase in water content, which leads to progressive warming of GST. Meltwater percolating to the ground surface or into talus matrices induces an extended isothermal phase at 0 °C known as the zero curtain and caused by release of latent heat during freezing (Outcalt et al., 1990). Spring snow disappearance date is signaled by an abrupt rise in temperatures accompanied with onset of high daily fluctuations. Number of snow days per cold season was estimated for the low talus surface positions at each site by selecting for and counting total days when daily standard deviations as modeled by GARCH analysis were <1.0 °C.

To compare proxy inferences about snow cover from temperature records with observed data, we extracted snow-depth time-series data from the USDA-NRCS SNOTEL records for Virginia Ridge (NRCS 2012). This site is located 5 km northeast and southeast, respectively, from the Virginia Cyn and Green Cr talus sites, and at an elevation (2804 m) 300 m below and above the mean elevation of our high and low elevation sites, respectively (Fig. 1, Table 1). The SNOTEL site lies on a small flat bench surrounded by tall lodgepole pine (*Pinus contorta*) forest and at a general northeast aspect.

Statistical analyses were conducted to assess differences in temperature by elevation, aspect, substrate, year, season, and talus position. Missing values were filled by imputation (SAS, 2011). Positions in the analysis were FAT, GST, TST, and TMT. Differences among means were tested by a standard least squares ANOVA, in JMP (SAS, 2011), with the six main effects, all two-way interactions, and the *season* × *position* × *elevation* interaction. In our analysis, all effects in the model were fixed.

TALUS HEAT TRANSFER

Heat transfer in taluses can occur via direct exchanges between talus and free air as well as indirectly through cold-air drainage, permafrost cooling (Kane et al., 2001), and other forms of meso- to micro-climatic circulation dependent on open lattice matrices of these landforms (Harris and Pedersen, 1998). Rather than apply heat transfer models used for soils, we chose to empirically explore matrix temperatures using transfer models of surface temperatures, following the approach of Millar et al. (2012). In that the temperature time series are autocorrelated,

statistical tests on standard regression models are not valid. Transfer-function modeling was done in the time series platform in JMP (SAS, 2011). We first detrended the data by autoregressive integrated moving-average (ARIMA) models. We then regressed linear, squared, and cubic terms of surface temperatures against the detrended matrix temperatures, detrending the surface temperature terms if necessary. Lags of 1–4 days were included to address delayed heat transfer from the surface to the matrix. Models were fit by minimizing AIC and SBC. In simpler, more direct representations of the resistance of matrix temperatures to changes in surface temperatures, we also fit the paired surface to matrix temperatures with cubic splines chosen to minimize higher frequency variation.

Results

MEAN ANNUAL AND SEASONAL TEMPERATURES

In the fixed effect model, all main effects except aspect were significant (unless otherwise noted below, all $p < 0.01$). Values of MAAT ranged from a low of –0.2 °C for high-elevation Virginia Cyn in 2011 to a high of 8.6 °C for low elevation Lee Vining Cyn in 2012 (Table 3). MAAT, mean annual minimum temperatures and mean annual maximum temperatures were significantly colder for high elevation sites than for low elevation sites. Whereas elevation was significant in the overall model, aspect was not. This appeared to be due to the inconsistent pattern of temperatures at low-elevation sites; at high elevations, north aspects were significantly colder than south aspects, whereas the reverse occurred at low elevations, creating a significant *elevation* × *aspect* interaction. Substrate had a significant effect, with metamorphic sites warmer than granitic sites. In measures of annual temperature, 2011 means were significantly colder than 2012. Overall, Virginia Cyn was consistently the coldest site, and Lee Vining Cyn was the warmest.

Freezing degree-days for 2011 and 2012 averaged –551 overall, with means of –844 for high elevation sites and –368 for low-elevation sites (Table 3). The average thawing degree-days for both years was 2138, with means of 1550 for high elevation sites and 2850 for low elevation sites. A plot of FI, TI, and isotherms at

TABLE 3

Mean annual average, minimum, and maximum temperatures of free air at 8 talus sites. Means given only for 2011 and 2012 water years, when data were complete. See Table 2 for abbreviations.

Talus site	Year	MAAT (°C)	Mean Tmin (°C)	Mean Tmax (°C)	FI (°C days)	TI (°C days)
Low-elevation sites						
Green Creek	2011	3.6	–1.1	9.3	–682	1991
	2012	6.2	0.3	13.2	–411	2691
Lundy Cyn South	2011	6.7	2.2	12.2	–356	2817
	2012	8.2	3.1	14.3	–257	3258
Lundy Cyn North	2011	6.2	1.8	10.7	–390	2635
	2012	7.5	2.7	12.5	–289	3038
Lee Vining Cyn	2011	7.3	3.0	11.9	–333	2985
	2012	8.6	4.1	13.6	–224	3390
Low Mean		6.8	2.0	12.2	–368	2850
SD		1.6	1.7	1.6	142	434
High-elevation sites						
Virginia Cyn	2011	–0.2	–3.5	3.2	–1178	1119*
	2012	3.0	–1.1	6.9	–794	1875
Saddlebag Lk	2011	1.4	–1.7	5.0	–936	1337
	2012	3.7	0.2	8.1	–584	1832
Warren Fork	2011	1.5	–1.1	4.9	–820	1386
	2012	3.3	–0.1	8.0	–649	1872
Greenstone Lk	2011	0.9	–3.1	4.7	–970	1300
	2012	2.3	–1.9	6.3	–824	1675
High Mean		2.0	–1.6	5.9	–844	1550
SD		1.3	1.3	1.7	187	298
Overall Mean		4.4	0.4	8.8	–551	2138
SD		1.5	2.3	3.9	331	847

*A month of data is missing in summer 2011.

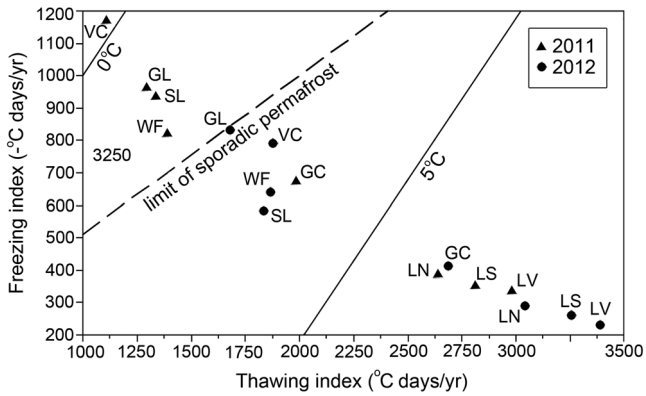

FIGURE 3. Relationship of eight talus sites to freezing index (FI), thawing index, and mean annual average temperature (MAAT) zones. The four low elevation sites were warmer than the 5 °C isotherm, three of the high elevation sites were within the 0–5 °C isotherm zone, and one site (Virginia Cyn) had MAAT colder than the 0 °C isotherm. Respectively, these are identified as no permafrost, sporadic permafrost, and discontinuous permafrost zones (Harris, 1981). Freezing indices, per Harris (1981), are plotted as (–1 × FI) °C.

critical temperatures for permafrost relations (sensu Harris, 1981) showed that in both 2011 and 2012 all low-elevation talus sites fell in Harris's zone of no permafrost (Fig. 3). In 2011, three of the high-elevation sites were in the zone of sporadic permafrost, and one (Virginia Cyn) was within the zone of discontinuous permafrost. In 2012, all high-elevation sites fell in the zone of no permafrost, although one (Greenstone Lake [Lk]) was just outside the limit of sporadic permafrost.

Considering temperatures by season (Table 4), mean cold-season air temperatures were consistently below freezing for the high elevation sites (mean, –2.1 °C), whereas all but one low elevation site (Green Cr) means were above freezing (mean, 2.2 °C). Interannual differences varied by position and season: 2011 was colder than 2012 for free-air temperature for cold and warm seasons, as well as for ground and talus means in the warm season. In the cold season, however, this order was reversed for ground and talus positions, with 2012 mostly colder. This is likely due to the low snow cover in 2012, which exposed thermochrons more often to winter air rather than insulation of deep snow. At all sites and years, talus matrix temperatures were colder than surfaces during the warm season. Ground-surface means were intermediate to TST and TMT, as were mean FATs. During the cold season, differences among the TST, TMT, and GST were nonsignificant; FATs were significantly colder. In the south-facing taluses, where data were complete for 2010, cold-season temperatures were colder in 2010 than in 2011 and 2012 for all positions; during the warm season, 2010 means were intermediate between those for 2011 and 2012. As in annual values, elevation was a significant factor for seasonal comparisons.

Fluctuations in diurnal temperatures, as indicated by standard deviations of mean temperatures, differed by position, elevation, and season (Table 5). Of interest were the significantly lower standard deviations for talus matrix temperature than surface or ground temperatures ($p < 0.05$). The contrasts were greatest in summer and autumn for all sites and years, and as well for spring at the low-elevation sites. During winter the contrasts were nonsignificant, and standard deviations were very low for talus and ground positions. This is interpreted as a snow-cover effect, in that the free-air positions had high diurnal fluctuations. In autumn and spring, the standard deviations of TST and TMT at high elevation sites were significantly lower ($p < 0.001$) than the values for respective positions at the low-elevation sites.

TEMPERATURE AND SNOW-COVER TIME SERIES

Trends across the eight taluses were consistent for FAT, GST, TST, TMT, and snow-cover characteristics. We summarize overall trends first, and then describe details below. Intra-talus correlations were high (>0.95) for all seasons and positions except winter, when spatially variable snow cover created thermal mosaics across the talus. Temperature time series from Saddlebag Lk and Green Cr (high and low sites, respectively) illustrate characteristic 2009–2012 patterns for TST, GST, and FAT (Figs. 4, parts A–D); time series from Saddlebag Lk illustrate comparisons of talus matrix, talus surface, and ground surface temperatures (Fig. 4, part E).

Significant patterns for the warm season included (all $p < 0.001$): (1) mean TMT and mean daily variances were lower than TST and lower than FAT; (2) low TST and TMT were colder (mean and minimum temperatures) than mid- and high-talus positions; (3) GST had greater daily extremes (minimum and maximum temperatures) than talus positions. Significant patterns existed for the cold season : (1) TMTs were warmer than TSTs. (2) Low TSTs were warmer than mid- and high-talus positions. The former more often persisted at 0 °C, while the latter fluctuated above and below freezing. (3) An isothermal zero-curtain period occurred before snow disappearance. (4) Snow covered the talus low positions and ground surface more often and longer seasonally than mid- and high-talus positions. (5) Snowpacks were greater at high-elevation sites than low-elevation sites. (6) Snowpacks were deepest (started and persisted longest) in winter of 2010–2011 and least in winter of 2011–2012.

Summer (1 June to 30 September)

To illustrate warm season patterns, summer temperatures are plotted for talus surface and matrix locations at the low, mid, and high talus positions for high-elevation Warren Fork (Fk) and low elevation Lundy North sites (Fig. 5). In each set of panel pairs, talus surface temperatures are in the upper panel and talus matrix temperatures in the lower. The contrast of lower mean temperature in matrix compared to surface is apparent, as is the attenuated variability in the matrix time series. For instance, at high elevation Warren Fk (Fig. 5, parts A–C), summer TST maximum temperatures were regularly above 25 °C and, especially in late summer, minima dipped near 0 °C. TMTs, by contrast, remained between 12 and 18 °C. The contrast was also strong in the low-elevation example (Lundy North, Fig. 5, parts D–F), where the matrix attenuation was particularly apparent in the low talus position in all years. The cooler temperatures in the low talus positions relative to mid and high positions were also documented for both TST and especially TMT. This contrast was particularly strong in the low-elevation taluses. Another consistent pattern illustrated is the late snowmelt date and lag in response to summer warm-up for the low talus positions, both surface and matrix. A final summer pattern was the abrupt late summer temperature declines, commonly in September, either through gradual lowering of means or periodic dips in temperature with reversals to mid-summer warmth.

Altitudinal temperature differentials (ATDs) further illustrate the pattern of temperatures relative to position on the taluses

TABLE 4

Mean seasonal temperatures of free air, ground surface, talus surfaces, and talus matrices. MCT is mean cold-season temperature (1 Oct to 31 May); MWT is mean warm-season temperature (1 Jun to 30 Sep). Mean air temperatures are from trees at 3.0 m above ground; ground surface means are from talus forefield postions; talus surface and talus matrix means are from low talus positions. Empty cells indicate incomplete data.

Talus site	Year	MCT Air (°C)	MCT Grd Surf (°C)	MCT Talus Surf (°C)	MCT Talus Matrix (°C)	MWT Air (°C)	MWT, Grd Surf (°C)	MWT Talus Surf (°C)	MWT Talus Matrix (°C)
Low-elevation sites									
Green Creek	2010		0.2	0.9	0.7		14.5	16.5	13.7
	2011	–1.2	0.5	1.1	1.5	13.1	13.5	15.9	12.2
	2012	1.7	0.6	1.6	1.5	15.2	14.2	16.7	14.4
Lundy Cyn South	2010		2.0	2.5	2.2		18.0	19.7	19.2
	2011	2.2	3.3	2.9	3.2	17.5	17.4	19.2	19.0
	2012	3.5	4.6	5.2	5.6	16.0	19.5	20.7	20.4
Lundy Cyn North	2011	1.8	0.4	0.5	0.5	15.0	15.5	15.1	12.0
	2012	3.2	0.9	0.1	0.0	16.1	16.9	17.1	13.9
Lee Vining Cyn	2011	2.6	2.2	2.4	2.3	16.5	17.6	18.9	16.8
	2012	3.8	3.5	3.3	2.4	18.2	19.6	20.4	17.8
Mean, Low		2.2	1.8	2.1	2.0	15.9	16.7	18.0	15.9
SD		1.6	1.6	1.5	1.6	1.6	2.2	2.0	3.1
High-elevation sites									
Virginia Cyn	2011	–4.0	–0.3	–0.9	–0.1	9.8	6.4	7.0	6.3
	2012	–1.5	–0.7	–1.6	–1.6	11.9	12.0	13.0	11.4
Saddlebag Lk	2010		–0.4	–1.2	–1.2		11.1	12.1	10.0
	2011	–2.9	1.8	1.3	1.3	10.0	9.0	10.5	8.3
	2012	–0.2	2.9	0.7	0.7	11.6	15.1	14.5	13.6
Warren Fork	2010		–0.3	–1.3	–0.6		9.4	10.5	9.1
	2011	–2.5	0.5	0.3	0.6	9.6	6.6	7.8	6.9
	2012	–0.7	0.8	0.1	0.0	11.5	13.6	13.7	12.4
Greenstone Lk	2011	–3.0	0.0	–0.5	–0.8	8.8	5.1	6.5	5.7
	2012	–1.9	–1.1	–1.7	–1.3	10.7	10.9	13.2	12.5
Mean, High		–2.1	0.3	–0.5	–0.3	10.5	9.9	10.9	9.6
SD		1.3	1.2	1.0	1.0	1.1	3.3	2.9	2.8
Overall Mean		0.3	1.1	0.9	0.9	12.7	12.9	14.1	12.5
SD		2.5	1.5	1.8	1.7	4.1	4.9	5.0	4.7

* A month of data are missing in summer 2011.

(Table 6). Summer differentials were strongly positive for all locations, with two exceptions (talus surface at Greenstone Lk in 2011 and Lee Vining Cyn in 2011 and 2012). Aside from these, mean ATDs ranged from 2 to 24 °C, indicating a strong flow, or pooling, of cool air downward over the surface of taluses and especially in talus matrices. ATD had larger positive values in summer at the low-elevation relative to high-elevation sites. Considered diurnally, ATD developed positive values at night, reaching maximum positive rates at midday. Positive values persisted into the afternoons and diminished by early evenings.

AUTUMN (1 OCTOBER TO 31 DECEMBER)

Cold-season patterns were more complex than summer trends as a result of snow cover, isolation of matrix from free air, and dynamics of freeze-thaw cycles. Figure 6 illustrates autumn temperature trends at a high- and low-elevation site for FAT, GST, and TST at low, mid, and high talus positions, and snow depth from the SNOTEL site. A common trend at all sites in late summer and early fall was for TST, TMT, and GST to become more coincident in amplitude with each other and with the FAT than earlier in summer, except that

TABLE 5

Standard deviations of mean temperatures by four seasons for free air, ground surface, talus surface, and talus matrix positions at high- and low-elevation sites. Summer is defined here as 1 Jun to 30 Sep; autumn as 1 Oct to 31 Dec; winter as 1 Jan to 31 Mar; and spring as 1 Apr to 31 May.

	Mean SD Low-elev. sites (°C)	Mean SD High-elev. sites (°C)
Summer		
Free Air	5.7	4.7
Ground Surface	6.2	6.8
Talus Surface	5.9	6.3
Talus Matrix	3.7	4.2
Autumn		
Free Air	6.7	5.8
Ground Surface	5.5	5.0
Talus Surface	6.0	4.8
Talus Matrix	4.8	3.3
Winter		
Free Air	5.4	5.2
Ground Surface	1.7	0.9
Talus Surface	2.0	1.1
Talus Matrix	1.5	0.8
Spring		
Free Air	6.4	5.7
Ground Surface	6.0	1.8
Talus Surface	6.2	2.1
Talus Matrix	4.4	1.5

TMT lagged the cooling TST. During the heavy snowpack year of 2010, autumn began with several light snowfall events as seen in the SNOTEL data and reflected in thermochrons (3 October and 7 November) at the high elevation site (Fig. 6, part A). The shallow snow cover in the first event, which melted at the SNOTEL site within a few days but persisted at the talus location, drove the FAT and talus temperatures to 0 °C, although the snow was shallow, as indicated by attenuated diurnal fluctuations. Shallow snow appears to have persisted, in particular at the low positions (ground surface and low talus), through to a large snowfall event on 20 November. Despite the deep snowpack, which started 20 November at the SNOTEL site, snow does not appear to have covered the high talus positions until 19 December, when SNOTEL snowpack doubled in depth to over 2 m. This is implied in temperatures on the high talus that dropped to –12 °C and persisted colder than –5° C through 19 December. After 19 December all thermochron positions except free air were under snow.

At the low-elevation Lundy South site in 2010 (Fig. 6, part C), no snow appears to have covered the talus or ground surfaces during the early events, as all positions showed high synchrony and amplitude until 20 November. At that time, snowpack deepened to 1 m at the SNOTEL site, snow covered the ground surface and low talus surface for about 2 weeks, and then it melted. As at the high-elevation site, at Lundy South, deep snow covered the entire talus and forefield ground surface after 19 December 2010.

Autumn of 2011 was dry and cold (Fig. 6, parts B and D). Two minor snow events occurred at almost the same time as in 2010 (4 October and 4 November), the first of which melted within a few days at the SNOTEL site. The first of these appears to have put snow on the ground surface and low talus positions for a few days at Virginia Cyn but not Lundy South. The second event brought snowpack to about 0.2 m at the SNOTEL site. At higher elevation Virginia Cyn, the ground surface was persistently snow-covered from 4 November onward. On the talus, however, only the low surface position was under snow, and this only for several weeks, until about 27 November, when snow melted. The middle and high TST through this period mirrored the FAT, with values often far below freezing, indicating snow-free conditions. After 27 November, all talus positions remained mostly below freezing through the end of the year. Talus positions often fluctuated daily and reached temperatures colder than –10 °C, indicating snow-free conditions.

At the low-elevation Lundy South site, in autumn 2011 (Fig. 6, part D), by contrast, the temperature patterns implied no snow cover on the talus or ground surface throughout autumn. All thermochrons followed a synchronous pattern with similar amplitudes, mirroring FAT.

Autumn altitudinal temperature differentials in the talus slopes were more variable than in summer among the sites and years (Table 6). In general, the low-elevation sites developed more positive values for talus surface and matrices than high-elevation sites, which had mixed negative and positive values.

Winter (1 January to 31 March)

The winters of 2011 and 2012 were very different at our talus sites (Fig. 7). Snowpacks at high-elevation sites, as indicated from SNOTEL data, were deep (>2 m) throughout winter of 2011, whereas snowpack in 2012 was only a trace amount until late January when the first significant snowfalls occurred. These accumulated to depths less than 1.2 m at the SNOTEL site through the season. Air temperatures at the high-elevation sites were mostly below freezing and fell commonly below –10 °C in both years; at low-elevation sites the same was true for 2011, but daytime temperatures were warmer and often above freezing in 2012. At both high and low elevation sites during winter 2011 (Fig. 7), GST and low TST remained at 0 °C throughout winter, with no daily fluctuation, indicating persistent snow cover at the talus base. At several other low-elevation sites (not shown), low snowpacks in winter 2012 delivered only trace amounts of snow cover on the taluses and forefields, as indicated by daily temperature variations above and below freezing, although with extremes more attenuated than free air.

Under heavy snowpacks of winter 2011, high and low elevation taluses illustrated an intra-talus altitudinal effect, with low positions warmest and higher positions colder. At Virginia Cyn (Fig. 7, part A), while the low talus surface temperature persisted at 0 °C, the mid position was –2 °C, and the high talus position was –4 to –5 °C. In winter 2012 at high and most low elevation sites, the low TST remained near 0 °C, and the mid and high TSTs generally were colder, with minima below –5 °C, and daily fluctuations above freezing. The latter followed the pattern of free air temperature although attenuated, indicating shallow snow cover.

Altitudinal temperature differentials in winter were dominantly negative at all high-elevation sites and the cold low-elevation site

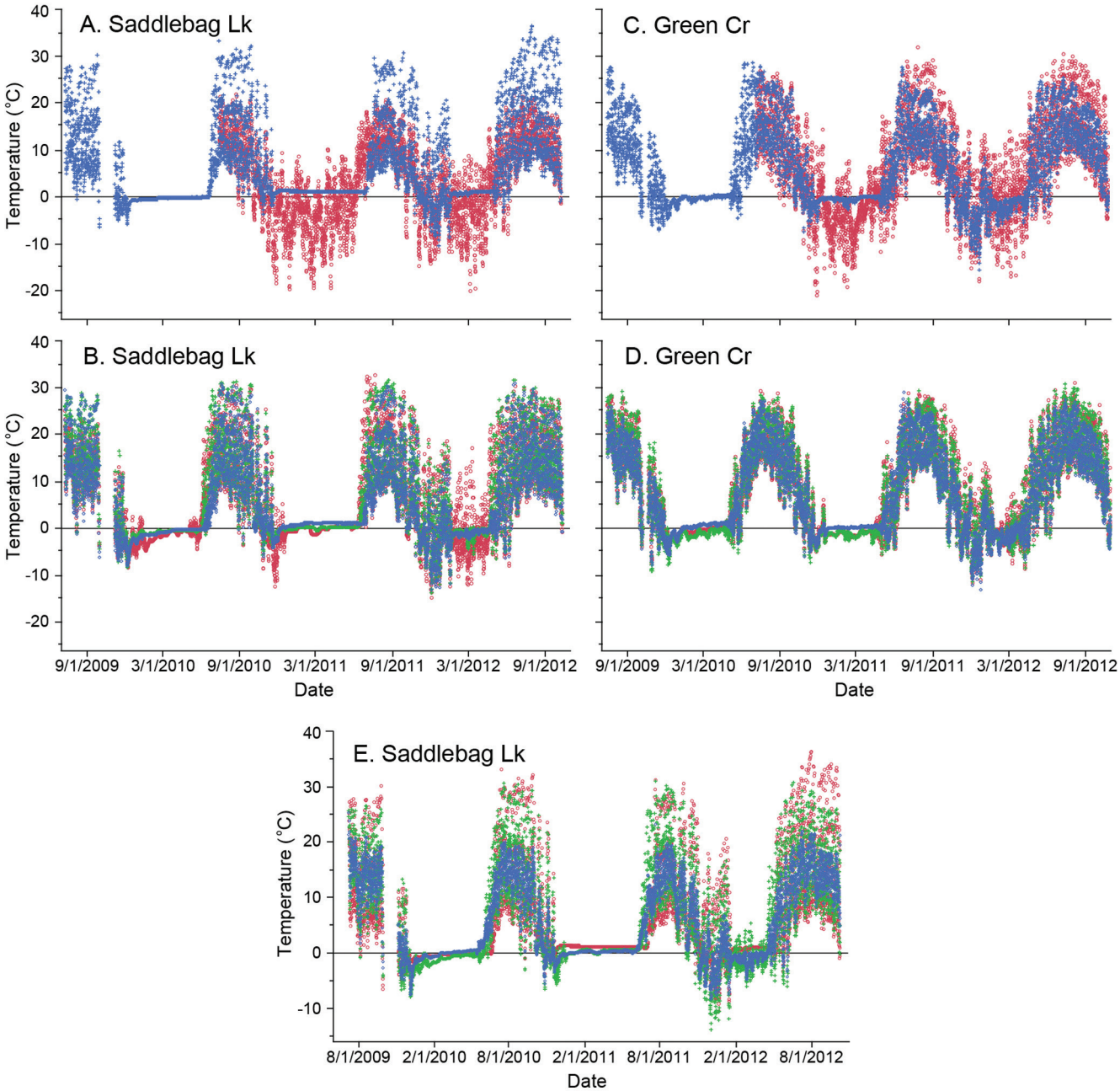

FIGURE 4. 2009–2012 time series temperature traces showing overview of annual and seasonal patterns. Results shown for a high elevation site (Saddlebag Lk, A–B) and a low elevation site (Green Cr, C–D). Free air (tree; red) and ground surface (forefield; blue) temperatures are shown in the top panel for each site (A, C) and talus surface for the low (blue), middle (green), and high (red) talus positions in the lower panel (B, D). A comparison of talus matrix (blue), talus surface (green), and ground surface (forefield; red) is shown for high elevation Saddlebag Lk site (E).

(Green Cr; Table 6). This was the case for all three winters and repeated the pattern of low talus surfaces being warmer in winter than higher surface positions, the reverse of the summer pattern. The other three low-elevation sites, by contrast, had generally positive ATDs in winter, indicating that the low surface positions were colder than areas higher in the taluses. In that these taluses had less snowpack than the high-elevation sites, heat transfer processes appear to have been similar to summer, suggesting the important role of snow in regulating talus winter thermal regimes.

Another common winter pattern was for the low talus matrix temperatures to be warmer than the low talus surfaces, another reversal from summer patterns. This is illustrated by high-elevation Saddlebag Lk (2010) and low-elevation Green Cr (2011; Fig. 7, parts E and F). In both cases, the low TMTs were significantly warmer than the low TSTs, a trend that became stronger as snowpack deepened over the sites. This was especially apparent at Green Cr, where the talus surface temperature persisted below 0 °C, while the matrices warmed above 0 °C after snowfall covered

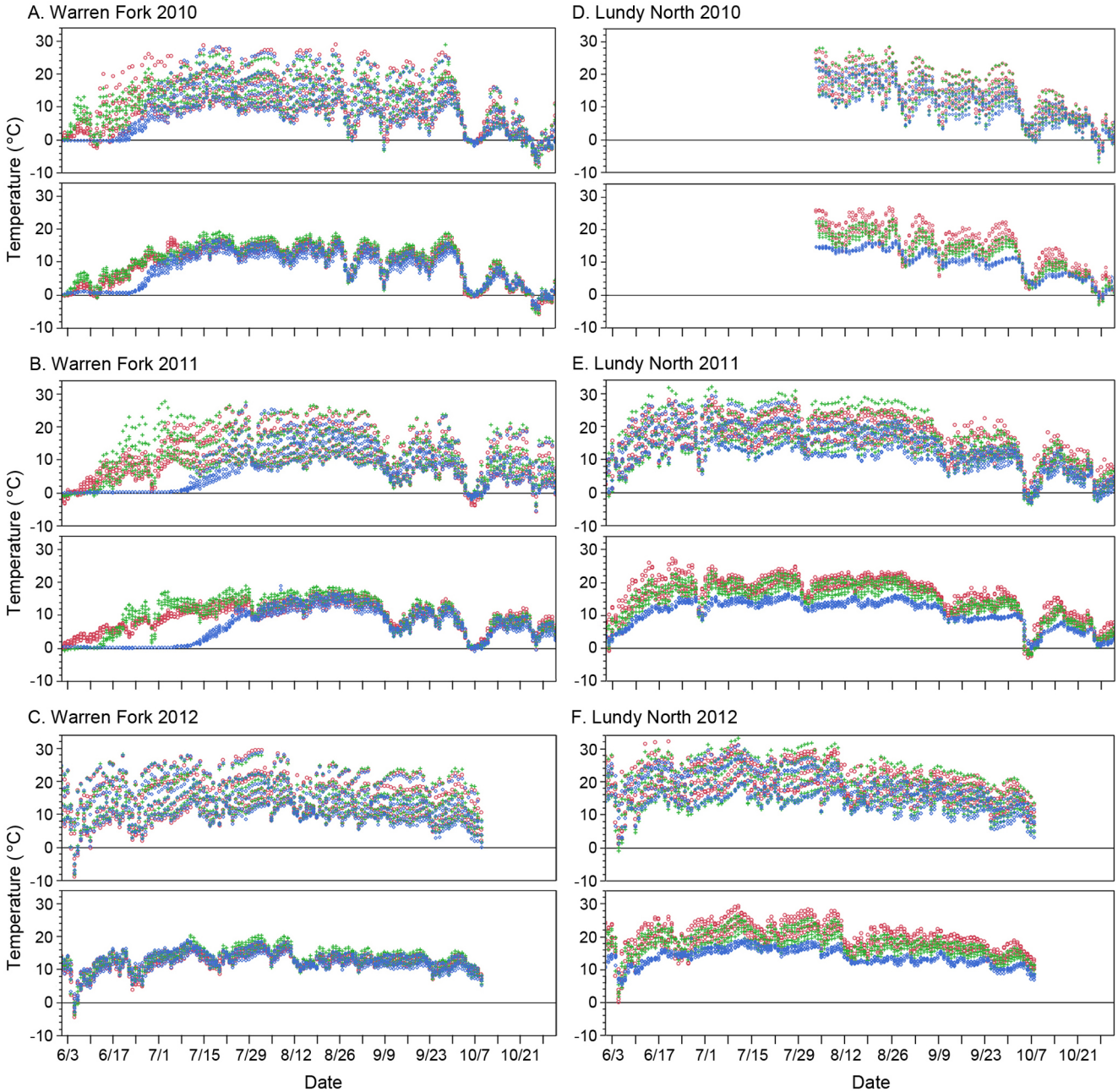

FIGURE 5. Summer time series temperature traces for a high elevation (Warren Fk, A–C) and a low elevation site (Lundy North, D–F), 2010–2012. In each pair, the upper panel shows talus surface temperatures, and the bottom panel shows talus matrix temperatures. In all cases, blue are low positions, green are middle positions, and red are high positions in the talus.

the site. The surface-matrix contrast was inconsistent at the mid- and high-talus positions.

Number of snow days estimated from the GARCH variance analysis confirmed the relationships indicated by the thermochrons about snow cover on the talus (Table 7). Significant interannual differences occurred as in other indicators, with winter 2011 having two to three times more snow days than 2012; 2010 was intermediate. The high-elevation sites had significantly more snow days than low-elevation sites ($p < 0.05$)—in most contrasts twice as many.

Spring (1 April to 31 May)

Temperature time series for spring showed declining snowpacks (high-elevation sites), snowmelt (low-elevation sites and dry years), and changing spatial relationships of snow cover on taluses (Fig. 8). At the high-elevation sites in all years, the ground surface and low talus surface remained at 0 °C beyond the time of snow disappearance at the SNOTEL site, and throughout spring at most sites except in 2012. The mid- and high-talus surface temperatures, by contrast, began to fluctuate diurnally

TABLE 6

Altitudinal temperature differentials (°C per 100 m) across talus surfaces and within matrix environment by season at eight locations and three years. Negative values indicate temperatures decline as elevation increases, while positive values indicate temperatures increase as elevation increases.

	High Elevation Sites (°C)								Low Elevation Sites (°C)							
	Warren Fk		Saddlebag Lk		Greenstone Lk		Virginia Cyn		Green Cr		Lundy South		Lundy North		Lee Vining Cyn	
Season/Yr	Surf	Mat	Surf	Mat	Surf	Mat	Surf	Mat	Surf	Mat	Surf	Mat	Surf	Mat	Surf	Mat
Summer																
2010	6.0	5.9	4.2	7.0					–1.7	10.8	1.8	1.9				
2011	12.0	11.2	9.2	10.2	–3.1	1.9	4.8	8.5	2.0	16.2	1.8	2.5	10.2	24.7	–2.6	6.9
2012	2.0	0.1	–0.2	–0.4	2.5	5.7	3.6	9.7	2.8	11.6	1.4	2.5	10.4	23.7	–3.9	9.5
Mean	**6.7**	**5.7**	**4.4**	**5.6**	**–0.3**	**3.8**	**4.2**	**9.1**	**1.0**	**12.9**	**1.7**	**2.3**	**10.3**	**24.2**	**–3.3**	**8.2**
Autumn																
2009	–0.2	–2.6	1.2	0.1					6.0	4.3	2.6	2.8				
2010	–1.2	–1.8	–4.3	–2.9	–1.2	–0.1	–8.4	–8.0	1.9	0.8	1.7	1.4	6.1	8.9	0.5	2.0
2011	1.6	2.8	8.5	6.7	–6.8	–6.8	–3.5	–4.7	15.4	6.3	4.1	4.1	9.6	7.1	–2.6	–0.4
Mean	**0.1**	**–0.5**	**1.8**	**1.3**	**–4.0**	**–3.5**	**–6.0**	**–6.4**	**7.8**	**3.8**	**2.8**	**2.8**	**7.9**	**8.0**	**–1.1**	**0.8**
Winter																
2010	–5.2	–6.5	–3.0	–3.8					–5.7	–1.5	2.1	1.4				
2011	–3.4	–4.1	–5.3	–7.0	–0.5	–0.1	–12.0	–11.3	–8.9	–10.3	0.8	0.2	3.9	4.0	2.2	0.9
2012	–4.1	–2.1	–1.1	–1.2	–6.5	–6.2	–8.9	–8.2	6.5	–3.7	2.0	2.9	8.9	4.9	0.1	0.9
Mean	**–4.2**	**–4.2**	**–3.1**	**–4.0**	**–3.5**	**–3.2**	**–10.5**	**–9.8**	**–2.7**	**–5.2**	**1.6**	**1.5**	**6.4**	**4.5**	**1.2**	**0.9**
Spring																
2010	–2.0	–2.3	–2.1	–4.7					–2.7	–0.9	0.4	0.6				
2011	–1.3	–2.8	–3.7	–5.8	–1.3	0.4	–3.3	–7.3	–0.1	–2.6	3.2	3.0	11.9	14.6	–0.8	3.4
2012	2.9	3.6	9.0	6.9	–1.1	–2.2	5.1	10.2	3.7	6.7	0.7	0.9	11.6	21.1	0.2	7.8
Mean	**–0.1**	**–0.5**	**1.1**	**–1.2**	**–1.2**	**–0.9**	**0.9**	**1.5**	**0.3**	**1.1**	**1.4**	**1.5**	**11.8**	**17.9**	**–0.3**	**5.6**

early in the season, tracking free-air temperature, and indicating snow-free conditions. At low-elevation sites, snowpack was transiently on and off the talus from early to mid-spring, as indicated by short periods of TST dropping to 0 °C, especially at the low position; in general the sites were snow-free much earlier than the SNOTEL site. In the case of Lundy South (Fig. 8, parts D–F), no snow at all appears to have covered the talus during spring in the dry year of 2012.

The isothermal condition known as zero curtain occurred in many of the spring time series. This indicated the onset of snowmelt through the snowpack, with the zero curtain ending when the talus became snow-free. In the case of Greenstone Lk in spring 2011, talus matrix temperatures and talus surface temperatures in early spring were –1.0 °C, and rose to 0 °C by late April, where they persisted until the talus was snow-free (Fig. 8, part G). At low-elevation sites (e.g., Lundy North in 2012; Fig. 8, part H), the zero curtain persisted briefly, with snow disappearance about 1 April. After snowmelt, the typical summer pattern set in, with talus matrices cooler than surfaces, attenuated variance in the matrix, and low talus positions cooler than high positions. However, increases in matrix temperature generally lagged those at the surfaces.

TALUS HEAT TRANSFER

The best models for exploring heat-transfer relationships between talus surface temperatures and talus matrix temperatures during the snow-free season required fitting autocorrelated and moving average effects, and in some cases removing the increasing or decreasing trend in temperature over the season. The models included linear, squared, and cubic terms of surface temperature, which gave fits of $R^2 > 0.95$. Patterns in surface-matrix relationships changed over the course of the warm season (Fig. 9). Spline fits of the diurnal-daily temperature surface-matrix pairs at Virginia Cyn for summer and fall temperatures in 2011 showed a 1:1 trend in matrix temperatures until surface temperatures reached about 8 °C (Fig. 9, part A). Matrix temperatures trended warmer than surface. Beyond that point, the rate of increase of matrix temperatures diminished notably with increased surface temperatures. There is also a suggestion of resistance to cooling below –5 °C. With the

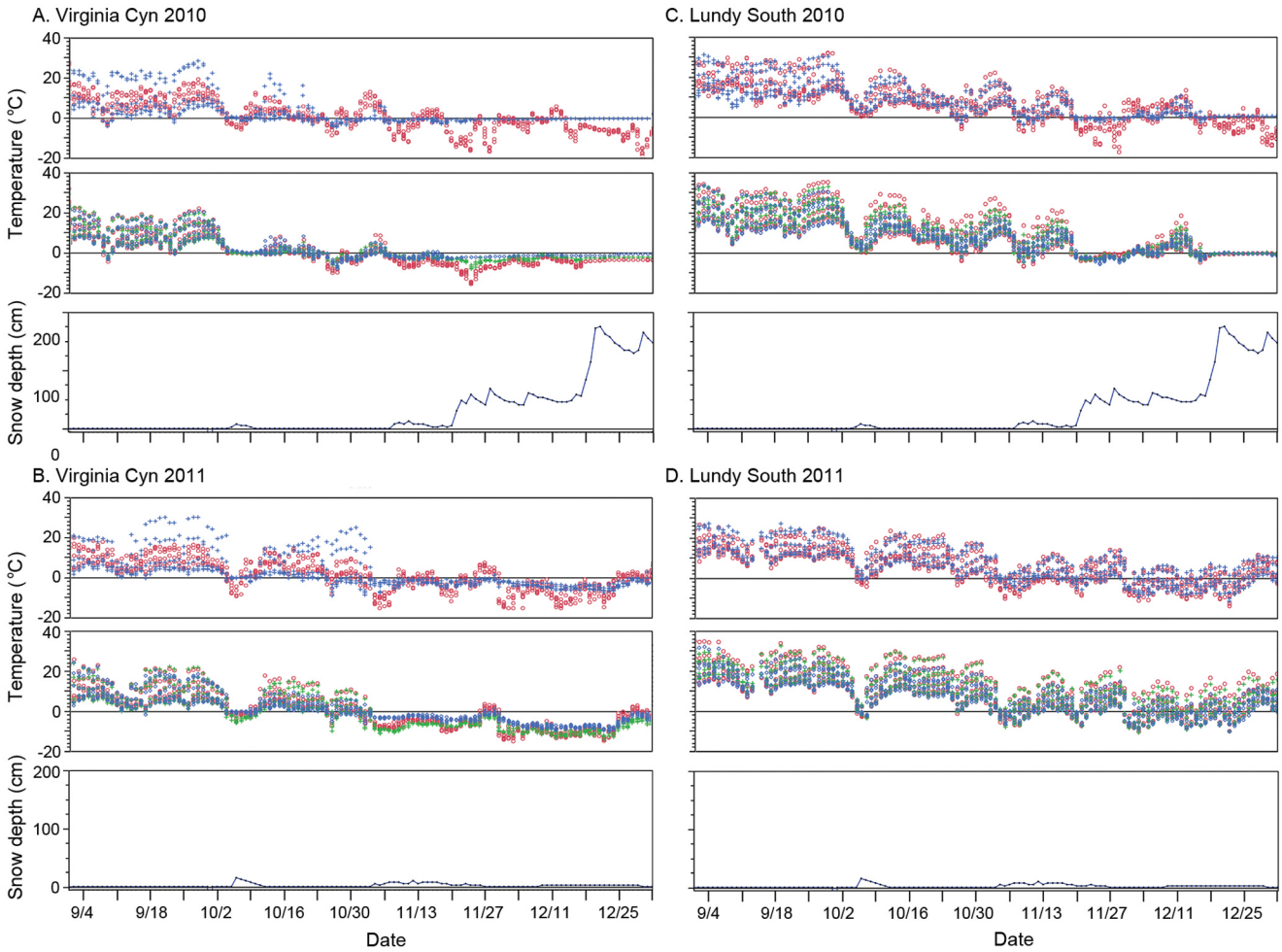

FIGURE 6. Autumn time series temperature traces for a high elevation (Virginia Cyn, A–B) and low elevation site (Lundy South, C–D), 2010–2011. In each trio, the upper panel shows ground surface (blue) and free air (red) temperatures, the middle panel shows talus surface temperatures (low, blue; mid, green; high, red), and the lower panel shows snowpack depth (blue) from the Virginia Ridge SNOTEL site.

reduced snow cover in winter and spring 2012, there was resistance to warming in the matrix temperatures throughout the entire range of surface temperatures (Fig. 9, part B). Because we removed the thermochrons early in October, we could not show the behavior of the data with cooling fall temperatures.

Lags at both surface and matrix were implied in the models (Appendix Fig. A1); TSTs were affected by air temperatures in prior days (1–4 days). Transfer functions of temperature data at all sites included the squared surface temperatures lagged by 1 day. In the matrix, resistance (hysteresis) to warming and cooling of the surface temperatures occurred within specific ranges of TST, and more often at the beginning and ending of the season than in the middle. In those times, matrix temperatures lagged 1–3 days in response to external changes. Free-air temperatures were in approximate weekly cycles of cooling and then rewarming: TMT would remain stable for 2–3 days, then respond to changes in TST, resulting in cycling behavior in the TMTs. Occasionally during these cycles, surface air cooled by as much as 10 °C, whereas matrices cooled by 3–8 °C, depending on the site. Subsequently, when TST switched to a warming pattern, TMT lagged several days then also warmed, but rose only to the mean of the past several weeks and no higher, despite warmer external temperatures. Matrix temperatures at Lundy South showed the least resistance to changes in surface temperatures; the regression slope of TST to TMT was about 0.90 every summer.

By late September to early October in all years, external air cooled rapidly and by as much as 10–13 °C. In these situations, matrix temperatures declined by about half the amount as external air, suggesting a partial loss of matrix resistance to cooling. Prior to significant snowfall accumulation (after mid to late November), even when surface temperatures would rise, matrix temperatures remained cool. With accumulation of snow on the talus, fluctuations in the matrix temperatures declined to trace, and the winter pattern set in.

Discussion

THERMAL PROCESSES

Thermal regions in coarse blocky ground have long been recognized to differ from those that occur in mineral soils or solid rock (Harris and Pedersen, 1998). This is due primarily to the relatively unimpeded air movement that is possible within

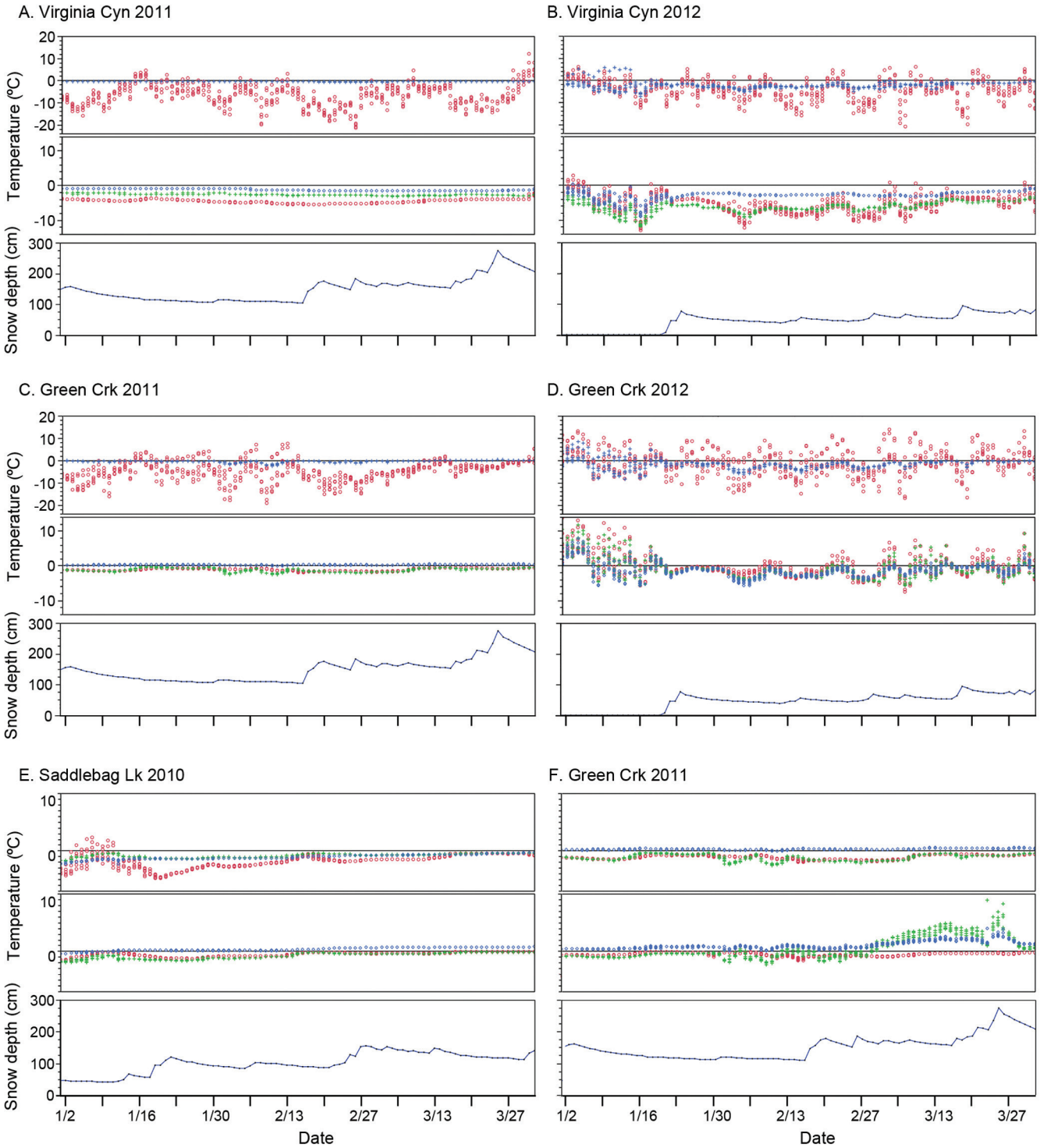

FIGURE 7. Wintertime series temperature traces showing contrasts for high and low elevation sites. (A–D) Comparisons at Virginia Cyn and Green Cr for 2011 and 2012 of ground surface (blue) with free air (red) temperatures (top panel); talus surface temperatures (low, blue; mid, green; high, red; middle panel); and snowpack depth (blue) from the Virginia Ridge SNOTEL site (low panel). (E–F) Comparisons at Saddlebag Lk (2010) and Green Cr (2011) of talus surface temperatures (low, blue; mid, green; high, red; upper panel), talus matrix temperatures (low, blue; mid, green; high, red; middle panel); and snowpack depth (blue) from the Virginia Ridge SNOTEL site (low panel).

the matrix lattice (open-air spaces) of these landforms as well as transfers between matrix and external air, which enables rapid heat exchange. When snow covers the blocky ground, circulation becomes impeded, with the degree depending on the depth, extent, and water content of the snow. A plethora of thermal processes, involving convection, advection, conduction, and

TABLE 7

Number of snow days at each location during winters of 2010–2011 for low- and high-elevation sites. Estimated from GARCH analysis for the low talus surface positions at each site. Dashes indicate years with no data.

	Year (# of snow days)		
Location	2010	2011	2012
Low-elevation sites			
Green Cr	149	157	46
Lundy South	83	100	0
Lundy North	—	176	74
Lee Vining Cyn	—	140	26
Mean	116	144	37
High-elevation sites			
Virginia Cyn	—	265	114
Saddlebag Lk	191	215	68
Warren Fk	198	243	108
Greenstone Lk	—	248	191
Mean	194	243	120

other heat-transfer mechanisms, has been proposed for blocky-ground landforms including rock glaciers, talus slopes, block fields, and subterranean caves (Table 8). The lack of consistent mechanisms in landforms having similar morphology suggests that the nature of heat transfer varies with many factors. Those most likely to influence thermal processes include environmental context (elevation, slope, aspect, substrate, clast size), ground thermal regime (permafrost and/or transient ground ice present or lacking), season (solar insolation and shading), and regional climate regime (mean temperature and snowpack abundance and water content).

Considering our high-elevation taluses, several thermal processes appear to be operating. Expectations for permafrost development in alpine zones are related to MAAT, GST evolution through winter, snow cover, and air exchange through snow. In alpine zones, discontinuous permafrost generally requires MAAT <0 °C, whereas sporadic permafrost, as under peat, in caves, and within blockfields and talus, can develop under specific environmental conditions where MAAT is as warm as 8 °C (Harris, 1981; Gude et al., 2003). Limiting factors as MAAT increases are related to FI and TI. Overall, MAATs of free air at our high-elevation sites were above freezing (mean, 2.0 °C), although one site in 2011 had MAAT –0.2 °C, yet several conditions suggested that persistent underground ice might occur. First, the 2011 freezing/thawing day indices (Fig. 3) indicated all high-elevation taluses to be within the zone assessed by Harris (1981) as either discontinuous or sporadic permafrost. Further, considering mid-winter periods where deep snow covered the thermochrons, all but two situations indicated talus surface and talus matrix temperatures at high talus positions to persist for several weeks between –2.0 and –5.0 °C, that is, within the range of winter equilibrium threshold temperatures where permafrost is expected in the Swiss Alps (Hoelzle et al., 1999). The exceptional cases were where snow cover was thin or lacking, in which case, winter equilibrium thresholds are not applicable, and at two sites (Saddlebag Lk and Warren Fk) where, in heavy snowpack winter of 2011, temperatures persisted between 0 and –2 °C. In all cases, temperature conditions suggesting permafrost occurred only in the upper talus areas, which, due to longer exposure to cold winter air (less snow), experience more extremes of cold winter temperature. Low positions, by contrast, were mostly snow-covered and remained warmer than –2.0 °C. In sum, tentative evidence suggests that persistent ice persists within the high-elevation talus slopes, contributing to the observed thermal regime. This finding is consistent with North American maps that indicate the Sierra Nevada to be within the zone of potential permafrost (Péwé, 1983; Harris, 1986), although highly sporadic.

Considering other processes potentially operating in the cold season (Table 8), cold-air drainage, Balch circulation, and chimney-flow ventilation are less likely in our taluses, as the Sierra talus temperatures were warmer at low positions than at mid and high positions, generating negative altitudinal temperature differentials. Further, low talus matrix temperature remained warmer than low talus surface, counterindicating thermal processes that involve dense cold air to sink. Further, the chimney effect does not seem to be operating, although transient conditions occur in late spring where warm air might exit high in the talus. Conduction via protruding rocks might operate in our high-elevation taluses, especially at high positions when snow was shallow. This would introduce attenuated diurnal fluctuations, occasionally observed in our time series at the mid- and high positions. Ice embedded in matrices might also have a role in transferring heat conductively, in that we often observed subsurface blocky ice and ice coating boulders in matrices long after surface snow disappeared. Continuous air exchange between talus matrix and surface when snow is lacking is also likely.

A final process that appears to operate during the late cold season in the high-elevation taluses is the zero curtain, caused by latent heat of freezing. A zero curtain extending from three to seven weeks occurred in 8 of 10 spring events at our taluses. The two exceptions, Saddlebag Lk in spring of 2011 and 2012, showed temperatures while snow-covered to remain between 0 and –1.0 °C, so a zero curtain, if it occurred during snowmelt, couldn't be discerned.

Warm-season conditions in the high-elevation taluses appear to be dominated by cold-air drainage combined with environmental effects within matrices of shading and internal air flow through the open lattices. These create cool conditions low in the talus (strong positive altitudinal temperature differentials), and cooler means and lower diurnal fluctuations in the matrix than talus surface. Lag effects and resistance of matrices to changes in surface temperatures counter-indicate equilibrium exchange with external free air, especially early and late in the season. In his original explanation of processes that support MAAT within blocky ground features and subterranean caves lower than MAAT of free air, Balch (1900) urged that regimes must be considered at annual not just seasonal scale. As Balch interpreted, cold winter air, due to its relative heavier density, is retained in caves and talus matrices well into the warm season, where further resistance to warming occurs due to shading, summer cold-air pooling, and the cooling effect of cold rocks on entering warm air. This seems likely to occur at our taluses, with added cooling due to latent heat adsorption from evaporation of water and ice in matrices and coating deep boulders as summer progressed. Supercooling (sensu Table 8) might also contribute to talus temperatures dropping below 0 °C in autumn, when abrupt cooling also occurred in external temperature and thin snow covered the talus.

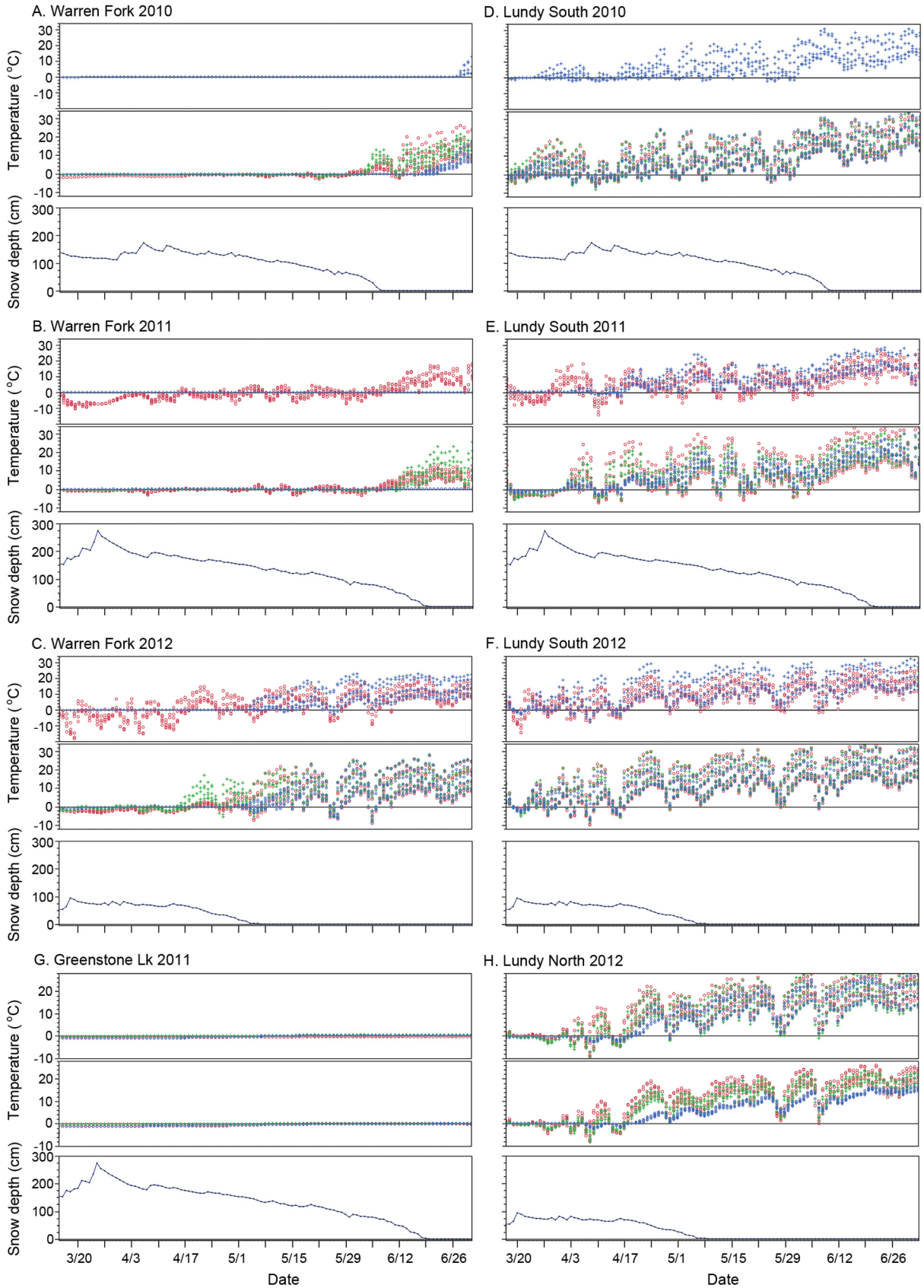

FIGURE 8. Springtime series temperature traces showing contrasts for high and low elevation sites. (A–F) Comparisons at Warren Fork and Lundy South for 2010–2012 of ground surface (blue) with free air (red) temperatures (top panel); talus surface temperatures (low, blue; mid, green; high, red; middle panel); and snowpack depth (blue) from the Virginia Ridge SNOTEL site (low panel). (G–H) Comparisons at Greenstone Lk (2011) and Lundy North (2012) of talus surface temperatures (low, blue; mid, green; high, red; upper panel), talus matrix temperatures (low, blue; mid, green; high, red; middle panel); and snowpack depth (blue) from the Virginia Ridge SNOTEL site (low panel).

TABLE 8

Thermal processes and conditions described in the literature that affect temperatures in coarse blocky landforms at annual and seasonal scales.

Annual
1. Environmental context (Brown, 1973; Haeberli, 1973; Hoelze et al., 1999; Lundquist et al., 2008). Environmental conditions including slope, aspect, canyon depth, and cirque topography affect thermal regimes through influence on solar radiation, solar insolation, snowpack accumulation (wind drift), depth, and retention. In the northern hemisphere, north aspects receive less insolation in winter and low angles of the sun penetrate the matrix of taluses on steep slopes more in winter than summer.
Warm Season
1. Continuous air exchange (convection; Harris and Pederson, 1998). The open lattice nature of coarse blocky ground promotes unimpeded air exchange between matrix and free air. Response of matrix air to warming or cooling of external air temperature can thus be rapid ("immediate"; Harris and Pederson, 1998). This effect is accelerated by wind at the landform surface (= forced convection; Kane et al., 2001), in which case it has been called wind-forced convection (Juliussen and Humlum, 2008) and also "wind holes" in Japan, when cold air blows out from voids between blocks at the base of the slope (Sasaki, 1986; Sawada et al., 2003).
2. Cold-air drainage (convection-advection; Haeberli, 1973; Hanson and Hoelzle, 2004). This common process at topo- to micro-spatial scales in mountainous regions (Whiteman et al., 1999; Whiteman, 2004) occurs in blocky ground when the difference between density of cold air (heavier) and warm air (lighter) forces cold air to flow downslope by gravity and pool at the base of slopes and in matrices. Cold-air drainage occurs when the air is windless and skies are clear, and, in typical mountain environments (i.e., canyon slopes), more often at night. A modification of the chimney-flow effect (see below) in summer involves cold-air drainage but adds a warming effect at the top of the blocky landform created as descending cold air within the matrix displaces a pool of warm air to the top of the feature (Harris and Pederson, 1998). When pockets of warm air ascend vertically and directly out to the surface rather than upslope as parallel advection, the effect is known as a heat bubble (Hanson and Hoelzle, 2004).
3. Balch circulation or effect (convection; Balch, 1900). Balch circulation is often cited as an explanation for ice in rocky caves and localized cold conditions in blocky landforms and is attributed to replacement of warm air with cold air due to density differences. This effect is not considered to be an equilibrium exchange with the atmosphere, and so a lag is expected for its development (Harris and Pederson, 1998). As originally described by Balch for subterranean caves, the process is more comprehensive than has been recited in the last 15 years. Balch attributed winter cold air to sink into caves (or talus matrices), and, due to density differences, to persist, excluding warm air. In summer, warm air penetration was resisted by density differences, and air that did enter (wind-pumping) was cooled as it encountered the cool interior. Such environments render MAATs colder than the surrounding means for ground temperature or free air and require air exchange at the top and bottom of the cave or matrix.
4. Evaporative and sublimation cooling (convection, vapor transfer; Von Wakonigg, 1996; Harris and Pederson, 1998). Evaporation and sublimation cause cooling due to the loss of more energetic (warmer) molecules that cool the evaporating surface or air space (latent heat adsorption). In blocky ground, ice often forms in the winter as a coating around boulders, which, during the warm season, evaporates or sublimates and causes matrices to cool. This process is most effective where summer air is dry.
5. Cold-season processes. Processes described below can occur in the warm season if snow-pack (≥ ~1 m) covers the talus for more than 1–2 days.
Cold Season
1. Warm-season processes. All of the processes above have been described as occurring in blocky landforms at times when no snow or shallow snow covers the surface.
2. Permafrost cooling (conduction/convection; Haeberli, 1973; Kane et al., 2001). The presence of permafrost within or below the bottom of blocky ground leads to evolution of matrix temperatures below 0 °C in late winter when heavy snowpack seals the matrix from air exchange with external free air. Threshold temperatures have been defined for the Swiss Alps (Hoelze et al., 1999): late winter/early spring matrix temperatures < –3 °C indicate talus over permafrost, whereas values > –2 °C indicate permafrost-free or inactive permafrost conditions (intermediate values are a range of uncertainty).
3. Chimney-flow ventilation or effect (advection; von Wakonigg, 1966; Sawada et al., 2002; Delaloye and Lambiel, 2005). Chimney-flow ventilation is also based on density differences between warm and cold air and is described as lateral upslope movement of warm air within matrices when deep snowpack covers the landform. Cold air enters through holes in the snowpack near the base of the landform, replacing less dense warmer air, which is displaced upslope and escapes at the top (higher elevation) or through snow funnels. This facilitates ground cooling, which can depress permafrost distribution as much as 1000 m below the regional limit.
4. Heat transfer via protruding rocks and ice (conduction; Sawada et al., 2003; Juliussen and Humlum, 2008). In semi-arid mountain regions, cold-season snowpack over blocky ground often does not completely cover the blocky ground. Rocks that protrude above the snowpack can conduct heat transfer between external free air and talus surfaces and matrix, serving as heat bridges to thermally couple the ground and air. Ice—either on rock surfaces or in matrices—can also serve as efficient bodies for conduction.
5. Latent heat of freezing, zero curtain (convection; Outcalt et al., 1990). Water from snowmelt in late winter/early spring flows onto the talus surface and into the matrix where it can encounter subfreezing temperatures below the snowpack. Re-freezing releases latent heat, which, as a continuous process during snowmelt, causes the temperature to persist uniformly near 0 °C. Once snowmelt ends (snow-free condition commences), the zero curtain is lifted.
6. Supercooling through shallow snow cover (Permanet, 2012). In late autumn and early winter, GST can cool as air temperature becomes negative, when snow cover is shallow. In these cases, overcooling may occur due to the high albedo of snow and the emission of long-wave radiation through the shallow snow.

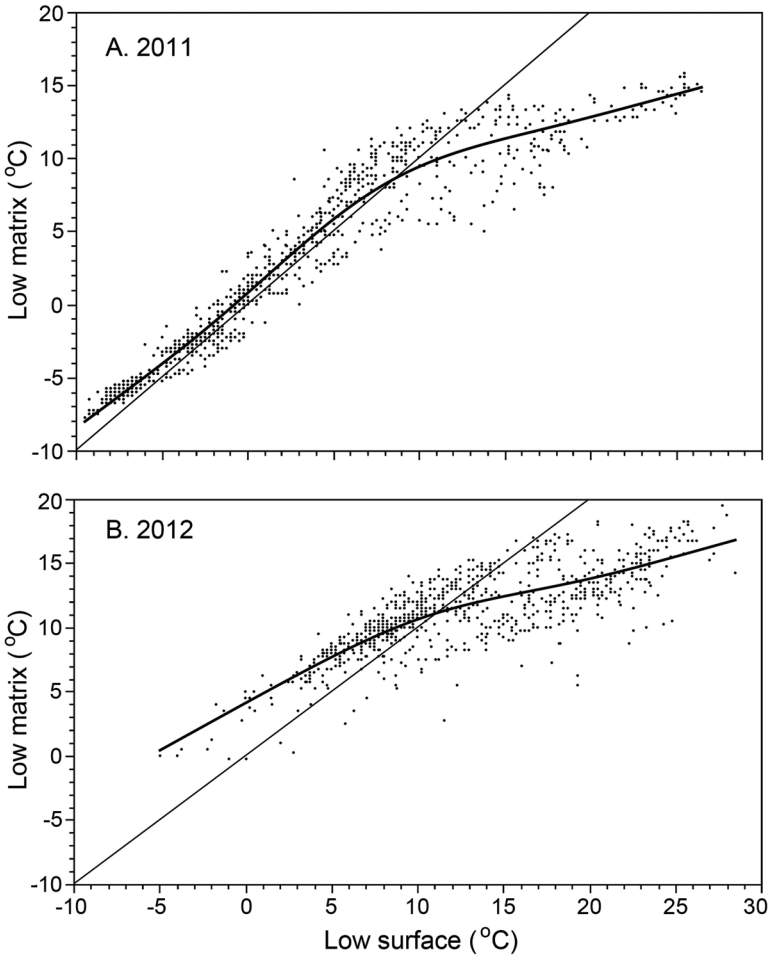

FIGURE 9. Response of matrix temperatures to surface temperature showing resistance of the matrix to warming and cooling. Dark curve is a spline fit to the data; light line indicates where equal temperatures in matrix and surface would lie. Virginia Cyn (high elevation site). (A) 2011 (1 June–31 December). (B) 2012 (1 June–8 October, when the experiment was terminated).

Thermal processes at the low-elevation taluses appear to be similar but simpler than at the high-elevation sites. These taluses very likely have no underlying permafrost or persistent ice, given MAAT of 6.8 °C and high late-winter equilibrium temperatures. In the cold season, the low-elevation taluses were variably covered by snow, and often snow-free, depending on site, aspect, and year; in all years, the higher talus positions were routinely snow-free. Warm-season (snow-free) patterns thus often developed in winter, with cold-air drainage and positive altitudinal temperature differentials. In situations with sufficient snowpack (2011), however, winter processes akin to the high-elevation taluses evolved, with negative ATDs and low positions warmer than high positions. As in the high-elevation sites, the latter was likely due to heavier snowpack insulating the lower portions of the talus, exposure of the high positions to external cold air, and lack of cold air drainage within the matrix. The zero curtain condition was less observed—or more difficult to discern—at the low-elevation sites than at the high, due to shallow or snow-free conditions or to temperatures persistent at 0 °C throughout winter.

The simplest explanation for warm-season thermal conditions at the low-elevation sites is cold-air drainage and Balch circulation combined with environmental conditions of shading in matrices and steep slopes further reducing solar radiation to the matrices. As at the high-elevation sites, thermal lags in response of matrix to surface conditions during the warm season best accords with sinking of heavy cold air to the talus base (low positions) rather than continuous air exchange with talus and free air. The Green Cr talus was a cold outlier among our low-elevation taluses, despite its south aspect, and behaved more like high-elevation taluses.

COMPARISON TO PREVIOUS STUDIES ON THERMAL REGIMES OF BLOCKY LANDFORMS

Although the literature is less well developed for talus slopes and block fields than for rock glaciers (Harris and Pedersen, 1998), a continuum exists of relative decoupling of the landform thermal regimes from ambient local climate (Ruzicka, 1993), with active rock glaciers and high-elevation cold-region taluses most decoupled, and relict rock glaciers and warm-region taluses least. In the Sierra Nevada, high-elevation, modern (likely ice-embedded; sensu Millar and Westfall, 2008) rock glaciers had consistent summer and winter thermal regimes (Millar et al., 2012) paralleling those described for rock glaciers elsewhere (e.g., Humlum, 1997; Bernhard et al., 1998; Hoelzle et al., 1999; Hanson and Hoelzle, 2004; Delaloye and Lambiel, 2005). The pattern of winter matrix temperatures in the Sierran rock glaciers, with persistent mid-winter temperatures below –4.0 °C terminating in spring with extensive isothermal zero curtain periods, indicates presence of permafrost. That likelihood

is corroborated by stable water flow at temperatures of ≤1 °C issuing year-round from springs.

Taluses have also been shown to be underlain by permafrost or persistent ice, although not before in the Sierra Nevada. In the Swiss Alps, a study of nine taluses within the alpine periglacial belt indicated permafrost beneath the talus (Lambiel and Pieracci, 2008). In these situations, permanent ice occurred at the lower portion of the talus. This was confirmed, including the lack of permafrost in the upper talus slopes, by analysis of electrical resistivity. Elsewhere in the Swiss Alp periglacial zone, borehole investigations revealed the presence of permafrost, where cooling was attributed to wintertime chimney flow ventilation made effective by heavy snow cover (Phillips et al., 2009). A final example from the periglacial belt of the Swiss Alps used thermal readings taken in talus boreholes to demonstrate that permafrost underlies the landform (Herz et al., 2003). The winter thermal time series at depth in the talus resembled typical patterns of permafrost rock glaciers in the Sierra Nevada and elsewhere, suggesting that similar thermal processes act in both rock glaciers and taluses of cold regions, although talus landforms are less consistent interannually in their cold regimes than rock glaciers.

At taluses within periglacial zones having drier climates and less consistent snowpack than the Swiss Alps, permafrost has been found to evolve under different heat transfer processes. In the Rocky Mountains of Alberta, for example, ground temperatures were 4–7 °C cooler in talus than adjacent soils, and permafrost occurred under talus (Harris and Pedersen, 1998). This was attributed to heat transfer by rapid air movement. At those locations, thermal coupling between free air and matrix was strong, with immediate responses of the matrix to changes in external temperatures, unlike the Sierra situation. Similarly, in a region of relatively low snowfall in central east Norway, talus mean annual ground temperatures were 1.3–2.0 °C colder than adjacent soils or bedrock, and permafrost underlay the blocky landforms (Juliussen and Humlum, 2008). This cooling was attributed to thermal coupling of the matrix with external cold winter air via conduction through boulders protruding above the snow.

Fewer studies have explored thermal regimes of talus slopes at elevations below the regional periglacial limit. In the Czech Republic of central Europe, low-elevation taluses, with MAAT of free air of 6–8 °C, were investigated (Gude et al., 2003; Zacharda et al., 2007). At these taluses, patchy permafrost was inferred to occur near the bases of the taluses, as those locations were the coldest positions year round, had time-series temperature patterns indicating permafrost, evolved zero curtain isotherm phases during snowmelt, and had talus matrix MAATs <0 °C. Negative thermal anomalies between matrix and free air temperatures were >4.6–9.0 °C. In Japan, permafrost was confirmed underlying alpine taluses below the regional periglacial zone where MAAT was 1.3–1.7 °C (Sawada et al., 2003) and elsewhere with MAATs above freezing (Ishikawa, 2003). Given relatively heavy snowpacks and positive ATD conditions during winter, chimney flow ventilation with wind-hole venting were interpreted as heat transfer mechanisms, although conduction via protruding boulders was also a factor.

Several commonalities and differences are apparent between the thermal regimes of Sierra Nevada taluses and those reported above. Although Sierran talus matrices were consistently and significantly cooler than talus surfaces in the warm season, as at other locations, they were by contrast warmer than the matrices in the cold season, balancing the differences at the annual scale, which was not noted in taluses elsewhere. Further, unlike situations where permafrost clearly developed under taluses, and talus temperatures were depressed as much as 7 °C from MAAT of free air, the contrasting seasonal differences in the Sierra taluses (matrices warmer than surface air in winter, cooler in summer) meant that the MAATs of talus and free air did not significantly differ. Cooler temperatures at the base of taluses in the warm season relative to higher positions were observed at all locations, but, unique to Sierran taluses, the reverse was the case in winter. Unlike the Sierra, most prior studies reported warmer air in winter in the upper talus sectors, implying chimney ventilation, which did not occur in the Sierran taluses.

We propose that the primary differences of our sites from those summarized above are due to the Mediterranean climates of the eastern Sierra Nevada, which have long, hot, and dry summers, and mild winters with relatively shallow snow-depths and short seasons. The snow-cover interpretations of Sierran taluses further indicate that snow accumulates at the bases but rapidly melts or doesn't accumulate on the upper talus portions. Thus, unlike regions of heavy winter snow, even in winter Sierran taluses are routinely only partially snow covered. In summer, Sierran talus matrices are cool and equable (attenuated extremes), most likely driven primarily by cold air drainage and possibly a lag effect from winter air penetration and Balch effect resistance to warming. In that persistent ice potentially underlies our high-elevation taluses, this promotes a milder thermal cooling than locations where permafrost is well-developed. Notwithstanding these differences, the internal thermal regimes of Sierran taluses, both high- and low-elevation sites, appear to be partly decoupled from ambient free air, with ATD values opposite in sign and orders of magnitude larger than that of free air in summer, large negative ATDs in winter, relative warmth in winter, and highly attenuated diurnal variations in summer.

TALUS AS THERMALLY BUFFERED HABITAT AND ECOLOGICAL REFUGIA—EXAMPLE OF AMERICAN PIKA

Changing global climates are affecting the quality of mountain ecosystems and catalyzing responses in species of high-elevation environments worldwide. In western North America, American pikas have become emblematic of concerns that mountain species, following synoptic temperature-lapse implications, will move upslope with warming, eventually running out of space, and that populations will be extirpated or go extinct. In that pikas are poor thermoregulators, nonhibernators, have short-distance dispersal capacity, and relatively low reproduction rates (Smith and Weston, 1990), they have been assessed as sensitive to 20th century changes and projected as especially vulnerable to future climate changes (Beever et al., 2003; Calkins et al., 2012). Counter to indications, however, and notwithstanding that some Nevada populations are in severe decline (Wilkening et al., 2011), pikas appear to be stable or thriving in locations across western North American mountains where they have been monitored (Hafner, 1994; Simpson, 2009; Millar and Westfall, 2010; Erb et al., 2011; Manning and Hagar, 2011; Stewart and Wright, 2012; Smith and Nagy, in review).

Pikas are highly restricted to talus habitat, usually foraging within a few meters from lower talus borders, and, other than during dispersal, remain active on talus surfaces and retreat to the matrix for shelter, escape from predations, and thermal protection (Smith, 1974; Smith and Weston, 1990). While general advantages of talus as mammalian habitat have long been observed, this study clarifies the extent to which talus habitats provide optimum thermal habitat for pikas, and potentially could buffer them and other species against challenges from warming in the future. In summer, talus matrices are cool and equable, with high and low

extremes well within the limits of physiological stress. Pikas preferentially remain near the low talus borders, which are the coolest position in the talus in summer. Forefields adjacent to the bases, where pikas forage, also have cool thermal conditions in summer, likely partly derived from cool air venting out the talus base. In winter, pikas abide near their cached food ("haypiles"), which they locate along the low talus border. These locations are the warmest portion of the talus in winter, remaining near 0 °C, and they are most likely of all talus positions to be snow-covered, thus further protected from severe winter temperatures and wind, as well as predation. The lesser snowpack of the upper talus portions, in contrast, provides pikas opportunity to escape the talus on warm days during winter and forage on species such as conifers, which have persistent foliage.

Conclusions

Results from our three-year study of thermal regimes of eight taluses at high and low elevations, north and south aspects, and contrasting substrate types in the central Sierra Nevada clarify annual and seasonal microclimate patterns and identify potential thermal processes operating in these blocky landforms. Primary among our findings for the warm season were that talus matrix mean temperatures and mean daily variances were lower than talus surface values and lower than free-air mean temperature; low talus surface and especially matrix positions were colder (mean and minimum temperatures) than mid and high talus positions, yielding very high positive altitudinal temperature differentials; ground surface had greater daily extremes (minimum and maximum temperatures) than talus positions; and talus matrix temperatures had significant lags (resistance) in response to surface temperature changes. The most likely processes contributing to these conditions were evaporative cooling in early summer, cold-air drainage and Balch effect throughout the warm season, potential supercooling in autumn, and combined shading and buffering effects of slope, substrate, and aspect.

Significant findings for the cold season were that talus matrices were warmer than talus surface positions (contrasting with warm-season conditions); low talus surfaces were warmer than mid and high talus positions—the former more often persisted at 0 °C, while the latter fluctuated above and below freezing (also opposite from summer); an isothermal zero-curtain period occurred before snow disappearance; snow covered the talus low positions and ground surface more often and longer than mid and high talus positions, which were often snow-free; snowpacks were greater at high-elevation sites than low-elevation sites; and snowpacks were deepest (started and persisted longest) in winter 2010–2011 and least in winter 2011–2012. Thermal processes most likely operating were insulation from snow cover at the talus bases, free exchange between talus matrix and external air in the upper talus portions, and latent heat from thaw-refreezing in late winter. The high-elevation taluses showed tentative evidence that permanent ice underlies the talus slopes. Only minor evidence existed for chimney-flow ventilation, commonly found in colder regions with more snowpack.

The thermal conditions found for these Sierra Nevada talus slopes indicate decoupling from ambient regional climates, especially in the warm season. As such, they develop unique microclimates that not only buffer winter cold and summer hot extremes, but spatially regulate portions of the talus. These conditions provide thermally buffered environments for mountain mammals that depend on taluses as habitat such as pikas, and are likely to be important refugial environments in the future.

Acknowledgments

We appreciate critical discussions about taluses and rock glaciers dynamics with Doug Clark (Western Washington University), Lin Liu (Stanford University), Jessica Lundquist and Nicoleta Cristea (both, University of Washington), a helpful review of the draft manuscript by Jessica Lundquist, and useful comments on the submitted manuscript from two anonymous reviewers.

References Cited

Balch, E. S., 1900: *Glacières or Freezing Caverns*. Philadelphia: Allen, Lane and Scott, 337 pp.

Barsch, D., 1996: *Rockglaciers. Indicators for the Present and Former Geoecology in High Mountain Environments*. Berlin: Springer Publishers, 331 pp.

Beever, E. A., Brussard, P., and Berger, J., 2003: Patterns of apparent extirpation among isolated populations of pikas (*Ochotona princeps*) in the Great Basin. *Journal of Mammalogy*, 84: 37–53.

Beniston, M., 2003: Climatic change in mountain regions: a review of possible impacts. *In* Diaz, H. (ed.), *Climate Variability and Change in High Elevation Regions: Past, Present & Future*. Dordrecht: Kluwer, 5–31.

Bernhard, L., Sutter, F., Haeberli, W., and Keller, F., 1998: Processes of snow/permafrost-interactions at a high mountain site, Murtel/Corvatsch, eastern Swiss Alps. Proceeding 7th International Conference on Permafrost, Yellowknife, Canada. Collection Nodicana. Sainte-Foy: Centre d'études nordiques, 35–41.

Brown, R. J. E., 1973: Influence of climatic and terrain factors on ground temperatures at three locations in the permafrost region of Canada. *In Second International Conference on Permafrost, Yakutsk*. Washington: National Academy Press, 27–34.

Calkins, M. T., Beever, E. A., Boykin, K. G., Frey, J. K., and Andersen, M. C., 2012: Not-so-splendid isolation: modeling climate-mediated range collapse of a montane mammal *Ochotona princeps* across numerous ecoregions. *Ecography,* 35: 780–791.

Chatfield, C., 2004: *The Analysis of Time Series. An Introduction*. Sixth edition. New York: Chapman & Hall/CRC Press.

Clark, D. H., Clark, M. M., and Gillespie, A. R., 1994: Debris-covered glaciers in the Sierra Nevada, California and their implications for snowline reconstruction. *Quaternary Research,* 41: 139–153.

Curry, A. M., and Morris, C. J., 2004: Late glacial and Holocene talus development and rockwall retreat on Mynyd Du, UK. *Geomorphology,* 58: 85–106.

Daly, C., Conklin, D. R., and Unsworth, M. H., 2009: Local atmospheric decoupling in complex topography alters climate change impacts. *International Journal of Climatology*, 30: 1857–1864, doi: http://dx.doi.org/10.1002/joc.2007.

Delaloye, R., and Lambiel, C., 2005: Evidence of winter ascending air circulation throughout talus slopes and rock glaciers situated in the lower belt of alpine discontinuous permafrost (Swiss Alps). *Norsk Geografisk Tidsskrift*, 59: 194–203.

Dobrowski, S. Z., 2010: A climatic basis for microrefugia: the influence of terrain on climate. *Global Change Biology*, 17: doi: http://dx.doi.org/10.1111/j.1365-2486.2010.02263.x.

Erb, L. P., Ray, C., and Guralnick, R., 2011: On the generality of a climate-mediated shift in the distribution of the American pika (*Ochotona princeps*). *Ecology,* 92: 1730–1735.

French, H. M., 2007: *The Periglacial Environment*. Third edition. Chichester: J. Wiley & Sons.

Friend, D. A., Phillips, F. M., Campbell, S. W., and Liu, T., 2000: Evolution of desert colluvial boulder slopes. *Geomorphology*, 36: 19–45.

Giardino, J. R., and Vitek, J. D., 1988: The significance of rock glaciers in the glacial-periglacial landscape continuum. *Journal of Quaternary Science,* 3: 97–103.

Gude, M., Dietrich, S., Mausbacher, R., Hauck, C., Molenda, R., Ruzicka, V., and Zacharda, M., 2003: Probable occurrence of sporadic permafrost in non-alpine scree slopes in central Europe. *In* Phillips, M., Springman, S. M., and Arenson, L. U. (eds.), *Permafrost*. Lisse: Swets and Zeitlinger, 331–336.

Haeberli, W., 1973: Die Basis-Temperatur der winterlichen Schneedeck als moeglicher Indikator fuer die Verbreitung von Permafrost in den Alpen. *Zeitschrift für Gletscherkunde und Glazialgeologie*, 9: 221–227.

Hafner, D. J., 1994: Pikas and permafrost: post-Wisconsin historical zoogeography of *Ochotona* in the Southern Rocky Mountains, USA. *Arctic and Alpine Research,* 26: 375–382.

Hanson, S., and Hoelzle, M., 2004: The thermal regime of the active layer at the Murtel rock glacier based on data from 2002. *Permafrost and Periglacial Processes,* 15: 273–282.

Harris, S. A., 1981: Climatic relationships of permafrost zones in areas of low snow-cover. *Arctic*, 34: 64–70.

Harris, S. A., 1986: Permafrost distribution, zonation and stability along the eastern ranges of the Cordillera of North America. *Arctic*, 39: 29–36.

Harris, S. A., and Pedersen, D. E., 1998: Thermal regimes beneath coarse blocky materials. *Permafrost and Periglacial Processes*, 9: 107–120.

Hayhoe, K., Cayan, D., Field, C. B., Frumhoff, P. C., Maurer, E. P., Miller, N. L., Moser, S. C., Schneider, S. H., Cahill, K. N., Cleland, E. E., Daleg, L., Drapek, R., Hanemann, R. M., Kalkstein, L. S., Lenihan, J., Lunch, C. K., Neilson, R. P., Sheridan, S. C., and Vervillee, J. H., 2004: Emissions pathways, climate change, and impacts on California. *Proceedings of the National Academy of Sciences of the United States*, 101: 12422–12427.

Herz, T., King, L., and Gubler, H., 2003: Microclimate within coarse debris of talus slopes in the alpine periglacial belt and its effect on permafrost. *In* Phillips, M., Springman, S. M., and Arenson, L. U. (eds.), *Permafrost*. Lisse: Swets and Zeitlinger, 383–387.

Hoelzle, M., Wegmann, M., and Krummenacher, B., 1999: Miniature temperature dataloggers for mapping and monitoring of permafrost in high mountain areas: first experience from the Swiss Alps. *Permafrost and Periglacial Processes*, 10: 113–124.

Humlum, O., 1997: Active layer thermal regime at three rock glaciers in Greenland. *Permafrost and Periglacial Processes*, 8: 383–408.

Ishikawa, M., 2003: Thermal regimes at the snow-ground interface and their implications for permafrost investigation. *Geomorphology*, 52: 105–120.

Juliussen, H., and Humlum, O., 2008: Thermal regime of openwork block fields on the mountains Elgahogna and Solen, central-eastern Norway. *Permafrost and Periglacial Processes*, 19: 1–18.

Kane, D. L., Hinkel, K. M., Goering, D. J., Hinzman, L. D., and Outcalt, S. I., 2001: Non-conductive heat transfer associated with frozen soils. *Global and Planetary Change,* 29: 275–292.

Kubat, K. (ed.), 2000: Stony debris ecosystems. *Acta Universitatis Purkynianae* 52, Studia Biologica, 202 pp.

Lambiel, C., and Pieracci, K., 2008: Permafrost distribution in talus slopes located within the alpine periglacial belt, Swiss Alps. *Permafrost and Periglacial Processes,* 19: 293–304.

Lundquist, J. D., and Cayan, D. R., 2007: Surface temperature patterns in complex terrain: daily variations and long-term change in the central Sierra Nevada, California. *Journal of Geophysical Research*, 112: D11124, doi: http://dx.doi.org/10.1029/2006JD007561.

Lundquist, J. D., and Lott, F., 2008: Using inexpensive temperature sensors to monitor the duration and heterogeneity of snow-covered areas. *Water Resources Research*, 44: doi: http://dx.doi.org/10.1029/2008WR007035.

Lundquist, J. D., Pepin, N., and Rochford, C., 2008: Automated algorithm for mapping regions of cold-air pooling in complex terrain. *Journal of Geophysical Research*, 113: doi: http://dx.doi.org/10.1029/2008JD009879.

Manning, T., and Hagar, J. C., 2011: Use of nonalpine anthropogenic habitats by American pikas (*Ochotona princeps*) in western Oregon. *Western North American Naturalist,* 71: 106–112.

Martinec, J., and Rango, A., 1986: Parameter values for snowmelt runoff modeling. *Journal of Hydrology*, 84: 197–219.

Millar, C. I., and Westfall, R. D., 2008: Rock glaciers and periglacial rock-ice features in the Sierra Nevada; classification, distribution, and climate relationships. *Quaternary International*, 188: 90–104.

Millar, C. I., and Westfall, R. D., 2010: Distribution and climate relationships of American pika (*Ochotona princeps*) in the Sierra Nevada and western Great Basin, USA; periglacial landforms as refugia in warming climates. *Arctic, Antarctic, and Alpine Research,* 42: 76–88.

Millar, C. I., Westfall, R. D., and Delany, D., 2012: Thermal and hydrologic attributes of rock glaciers and periglacial talus landforms; Sierra Nevada, California, USA. *Quaternary International,* 310: 169–180, doi: http://dx.doi.org/10.1016/j.quaint.2012.07.019.

Millar, C. I., Westfall, R. D., Evenden, A., Holmquist, J. G., Schmidt-Gengenbach, J. R., Franklin, R. S., Nachlinger, J., and Delany, D. L., 2014: Potential climatic refugia in semi-arid, temperate mountains: Plant and arthropod assemblages associated with rock glaciers, talus slopes, and their forefield wetlands, Sierra Nevada, California, USA. *Quaternary International*: doi: http://dx.doi.org/10.1016/j.quaint.2013.11.003.

NRCS [National Resources Conservation Service], 2012: National Climate and Water Center. California SNOTEL sites. <http://www.wcc.nrcs.usda.gov/snotel/California/california.html>.

Outcalt, S. I., Nelson, F. E., and Hinkel, K. M., 1990: The zero-curtain effect: heat and mass transfer across an isothermal region in freezing soil. *Water Resources Research*, 26: 1509–1516.

Parmesan, C., and Yohe, J., 2003: A globally coherent fingerprint of climate change impacts across natural systems. *Nature*, 421: 37–42.

Permanet, 2012: PermaNET—Longterm Permafrost Monitoring Network. <http://www.permanet-alpinespace.eu/>.

Pepin, N., and Lundquist, J. D., 2008: Temperature trends at high elevations: patterns across the globe. *Geophysical Research Letters*, 35: L14701, doi: http://dx.doi.org/10.1029/2008GL034026.

Péwé, T. L., 1983: Alpine permafrost in the contiguous United States: a review. *Arctic and Alpine Research*, 15: 145–156.

Phillips, M., Zenklusen Mutter, E., Kern-Luetschg, M., and Lehning, M., 2009: Rapid degradation of ground ice in a ventilated talus slope: Fluela Pass, Swiss Alps. *Permafrost and Periglacial Processes,* 20: 1–14.

Ruzicka, V., 1993: Stony debris ecosystems—Sources of landscape diversity. *Ekologia,* 12: 292–298.

SAS, 2011: JMP 9.01. Cary, North Carolina: SAS Institute Inc.

Sasaki, H., 1986: Air and soil temperature affecting the distribution of plants on a wind-hole site. *Ecological Review,* 21: 21–27.

Sass, O., 2006: Determination of the internal structure of alpine talus deposits using different geophysical methods (Lechtaler Alps, Austria). *Geomorphology*, 80: 45–58.

Sawada, Y., Ishikawa, M., and Ono, Y., 2003: Thermal regime of sporadic permafrost in a block slope on Mt. Nishi-Nupukaushinupuri, Hokkaido Island, northern Japan. *Geomorphology*, 52: 121–130.

Simpson, W. G., 2009: American pikas inhabit low-elevation sites outside the species' previously described bioclimatic envelope. *Western North American Naturalist,* 69: 243–250.

Smith, A. T., 1974: Distribution and dispersal of pikas. Influence of behavior and climate. *Ecology*, 55: 1368–1376.

Smith, A. T., and Nagy, J. D., in review: Population resilience in an American pika (*Ochotona princeps*) metapopulation. *PLoS ONE*.

Smith, A. T., and Weston, M. L., 1990: Mammalian species, *Ochotona princeps*. *American Society of Mammalogists,* 352: 1–8.

Stewart, S. A. E., and Wright, D. H., 2012: Persistence and apparent extirpation of American pika at northern Sierra Nevada historic localities. *Wildlife Society Bulletin,* 36: 759–764.

Thuiller, W., Lavorel, S., Araujo, M. B., Sykes, M. T., and Prentice, I. C., 2005. Climate change threats to plant diversity in Europe. *Proceedings of the National Academy of Sciences of the United States*, 102: 8071–8072.

Von Wakonigg, H., 1996: Unterkuehlte Schutthalden. *Arbeiten aus dem Institut für Geographie der Karl-Franzens-Universität Graz*, 33: 209–223.

Washburn, A. L., 1956: Classification of patterned ground and review of suggested origins. *Bulletin of the Geological Society of America*, 67: 823–866.

Washburn, A. L., 1980: *Geocryology: a Survey of Periglacial Processes and Environments*. New York: Wiley Publishers. 406 pp.

White, S. E., 1981: Alpine mass movement forms (noncatastrophic): classification, description, and significance. *Arctic and Alpine Research,* 13: 127–137.

Whiteman, C. D., 2004: Inversion breakup in small rocky mountain and alpine basins. *Journal of Applied Meteorology,* 43: 1069–1082.

Whiteman, C. D., Bian, X., and Zhong, S., 1999: Wintertime evolution of the temperature inversion in the Colorado Plateau Basin. *Journal of Applied Meteorology*, 38: 1103–1117.

Wilkening, J. L., Ray, C., Beever, E. A., and Brussard, P. F., 2011: Modeling contemporary range retraction in Great Basin pikas (*Ochotona princeps*) using data on microclimate and microhabitat. *Quaternary International,* 235: 77–88.

Zacharda, M., Gude, M., and Růžička, V., 2007: Thermal regime of three low elevation scree slopes in central Europe. *Permafrost and Periglacial Processes*, 18: 301–308.

MS accepted November 2013

APPENDIX

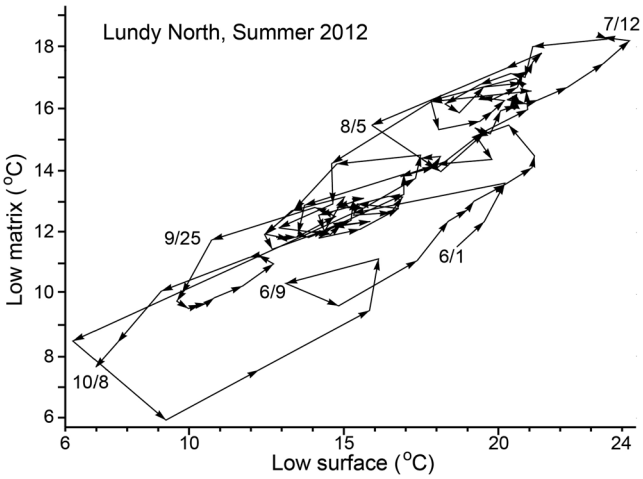

FIGURE A1. Time series model (ARIMA) for Lundy Cyn (Canyon) North talus showing response of talus matrix temperatures to changes in talus surface temperatures during the warm season of 2012. Dates show the progression of temperatures over the season.